arXiv:1302.2609v3 [physics.atom-ph] 11 Mar 2013

Non-adiabatic Coulomb effects in strong field ionisation in circularly polarised laser fields I: Ionisation rates

Jivesh Kaushal and Olga Smirnova

Max Born Institute, Max Born Strasse 2a, 12489 Berlin, Germany

Abstract

We develop the recently proposed analytical R-matrix (ARM) method to encompass strong field ionisation by circularly polarised fields, for atoms with arbitrary binding potentials. Through ARM, the effect of the potential can now be included consistently both during and after ionisation, providing a complete picture for the effects of the long-range potential. We find that the Coulomb effects modify the ionisation dynamics in several ways, including modification of (i) the ionisation (exit) times, (ii) the initial conditions for the electron continuum dynamics, (iii) the "tunnelling angle", at which the electron "enters" the barrier, and (iv) the electron drift momentum. We derive analytical expressions for the Coulomb-corrected ionisation times, initial velocities, momentum shifts and ionisation rates in circularly polarised fields, for arbitrary angular momentum of the initial state. We also analyse how the non-adiabatic Coulomb effects modify (i) the calibration of the attoclock in the angular streaking method, and (ii) the ratio of ionisation rates from p^- and p^+ orbitals.

PACS numbers: 32.80.Rm, 42.50.Hz, 33.80.Wz

I. INTRODUCTION

Single and double ionisation in circularly polarised strong laser fields is a sensitive probe of attosecond dynamics [1–6]. Strong field ionisation is often viewed as electron tunnelling from atoms and molecules through the barrier created by the laser field and the core potential. The adiabatic approximation, frequently used to describe tunnelling, implies quasi-static electric field and zero electron velocity immediately after ionisation (at the tunnel exit). This adiabatic picture is used for the interpretation of current experiments in circularly polarised laser fields [1–6] within the two-step model. This model merges quantum and classical approaches by combining (i) the adiabatic approximation for the quantum ionisation step with (ii) the classical trajectories calculation after tunnelling. In this second step, an ensemble of classical trajectories is launched outside the barrier; the distribution of initial velocities parallel and perpendicular to the direction of the instantaneous laser field is centered around zero, as predicted by the adiabatic tunnelling theory.

However, strictly speaking, in circularly polarised laser fields the tunnelling barrier is rotating. This rotation manifests itself in the non-adiabatic electron response, which becomes significant in the regime of the Keldysh parameter $\gamma \geq 1$. Non-adiabatic effects change tunelling from essentially one-dimensional, characteristic of the static limit [4, 7], to two-dimensional. As shown in [8], for short-range potentials substantial deviations from the adiabatic approximation arise already for $\gamma^2 \simeq 0.5$, which also questions the validity of this approximation for the long-range core potentials under similar conditions. We note that $\gamma^2 \simeq 0.5$ is a typical regime for recent experiments with laser radiation around 1600-1300 nm and systems with ionisation potential $I_p \sim 10$ eV (see e.g. [9]).

Here we provide rigorous analytical framework for treating the effects of long-range potential and laser field on equal footing and include non-adiabatic effects due to the long range potential. In particular, we show that non-adiabatic Coulomb effects lead to non-zero initial velocity both parallel and perpendicular to the direction of the instantaneous laser field even for the central electron trajectory (for which the ionisation rate maximises), when it emerges from the classically forbidden region.

We find that the non-adiabatic Coulomb effects modify the ionisation dynamics in several ways, including modification of (i) the ionisation (exit) times, (ii) the initial conditions for electron continuum dynamics, (iii) the "tunnelling angle", at which the electron "enters"

the barrier, and (iv) the electron drift momentum. We derive analytical expressions for the ionisation times, initial velocities, momentum shifts and ionisation rates in circularly polarised fields for arbitrary angular momentum of the initial state. We also analyse how the non-adiabatic Coulomb effects modify (i) the calibration of the attoclock in the angular streaking method, and (ii) the ratio of ionisation rates from p^- and p^+ orbitals obtained for short range potentials in [8].

Our tool is the gauge-invariant, analytical R-matrix-type method (ARM), which we have recently developed [10] for linearly polarised fields. The strength of ARM is the ability to treat consistently the effects of long-range potential and the laser field [10] as well as multielectron effects [11]. The main idea of the method was adopted from the study of collision processes and nuclear resonance reactions [12], where the primary purpose was to isolate the strongly interacting kernel from the region where these interactions were significantly weaker, and can be considered in asymptotic approximation. In this sense, the R-matrix approach developed in collision physics meets a crucial requirement of strong field physics, in that it can be used to separate the region of the configuration space where the Coulomb forces are much stronger than the laser field, from the outer region where the Coulomb potential quickly becomes almost negligible compared to the driving laser field. We note that fully numerical time-dependent R-matrix approach for strong-field dynamics has been developed and successfully applied in [13].

In [10], detailed analysis and benchmarking of the ARM method was provided for strong linearly polarised laser fields, including the derivation of analytical results for the instantaneous ionisation amplitudes and the sub-cycle ionisation rates for single active electron systems. With suitable approximations, the results for the cycle-averaged ionisation rates from [10] agree with those obtained by Perelomov, Popov and Terentév (PPT) [14]. For hydrogen-like atoms and ions, the PPT rates (with the new correction factor derived in [15]) were shown to be accurate for arbitrary values of the Keldysh parameter.

The difference between our problem in circularly polarised fields and the case of the linearly polarised fields analysed in [10] lies in the fundamentally two-dimensional character of tunnelling, i.e. the time-varying angles between the position vectors, the electron velocity $\mathbf{v_p}(t)$, and the laser vector potential $\mathbf{A}(t)$. As a consequence, certain approximations in [10] that were helpful in deriving physically transparent solution for the linearly polarised field are not always adequate in the case of circularly polarised fields. Here, we refine the ARM

method and extend it to the strong circularly polarised fields. We show that an appropriate choice of the the boundary between inner and outer region allows one to build the hierarchy of interactions and show how the long-range effects can be included consistently within the iterative approach.

Our strategy can be summarised as follows. Following [10], we introduce the "R-matrix" sphere of radius a, which splits the configuration space into the inner and outer regions.

A. The inner region: In the inner region the Coulomb field dominates, and the effects of the laser field on the inner region wave-function can be included in the quasistatic approximation. Further approximation, such as using the field-free wave-function is justified for fields significantly smaller than κ^3, where $\kappa = \sqrt{2I_p}$, I_p is the ionisation potential.

B. The boundary: The Bloch operator is used to "pass" the information about the electron wave-function from the inner region to the outer region. The outer region Green's function is used to propagate the outer region wave-function from this boundary to the detector. The boundary value is given by the inner region wave-function at the surface of the "R-matrix" sphere. Boundary matching ensures that the final result does not depend on the choice of the boundary value a.

C. The outer region: In the outer region, the Coulomb potential is weak and can be included in the Eikonal-Volkov approximation (EVA) [16]. It has been shown previously [17], that the Eikonal-Volkov approximation is adequate for the soft-core potentials, i.e. for the long-range potentials outside the singularity region.

D. Propagation in the outer region: involves integration over the surface of the R-matrix sphere (θ', ϕ') and over all times (t') of "transition" through the boundary. Due to the large action S of the electron in the strong laser field, the integrals are taken from highly oscillating function $P(\theta', \phi', t')e^{iS(\theta', \phi', t')}$ and are accumulated in the vicinity of their respective stationary (saddle) points θ'_s, ϕ'_s, t'_s, defined by the solutions of equations $S_{\theta'} = 0$, $S_{\phi'} = 0$, and $S_{t'} = 0$ respectively, where the subscript denotes derivative w.r.t. that variable. The action is given by $S = S^{\rm SFA} + G_C$, where the SFA (Strong Field Approximation) action is associated with the dynamics in the laser field and short range potential, and G_C is the action associated with the interaction

with the long-range potential of the core under EVA [16] and describes Coulomb-laser coupling [18]. Since only a vicinity of saddle points contributes to the integral, we make Taylor expansion of G_C around SFA saddle points $\theta_s'^{(0)}$, $\phi_s'^{(0)}$ and $t_s'^{(0)}$. After this expansion the integral over the sphere surface is calculated exactly. The integral over t' is evaluated using the saddle point method. The actual, full saddle point t_s' (shifted from $t_s'^{(0)}$ due to long-range effects) is found within the iterative approach. Formally, non-adiabatic effects in ionisation rates arise due to the deviations from the stationary trajectory included via Taylor expansion of G_C. Non-adiabatic coulomb effects also manifest itself in the photoelectron spectra and will be considered in our subsequent paper [19].

E. Iterative approach to saddle point equation for t': By construction, in the outer region G_C presents a perturbation to the SFA action $S^{\rm SFA}$ and therefore can only slightly shift the SFA saddle point $t_s'^{(0)}$, which correspond to the stationary SFA action: $\partial_{t'} S^{\rm SFA} = 0$. Thus, as a first correction to the saddle point, due to the interaction with the long-range potential $t_s'^{(1)} = t_s'^{(0)} + \Delta t_s'^{(0)}$, where $\Delta t_s'^{(0)}$ can be found by iterations with respect to G_C. The first iteration includes only linear terms in $\Delta t_s'^{(0)} \sim G_C$. In our approach we keep only the first-order correction terms consistently throughout. The saddle point equation $S_{t'} = 0$ can be expanded around $t_s'^{(0)}$: $\partial_{t'} S^{\rm SFA}\left(t_s'^{(0)}\right) + \Delta t_s'^{(0)} \partial_{t'}^2 S^{\rm SFA}\left(t_s'^{(0)}\right) + \partial_{t'} G_C\left(t_s'^{(0)}\right) = 0$, yielding $\Delta t_s'^{(0)} = -\frac{\partial_{t'} G_C\left(t_s'^{(0)}\right)}{\partial_{t'}^2 S^{\rm SFA}\left(t_s'^{(0)}\right)}$. Note that since the SFA action is stationary $\partial_{t'} S^{\rm SFA}\left(t_s'^{(0)}\right) = 0$, the shift due to $\Delta t_s'^{(0)}$ will only change the value of the SFA action in the second order wrt G_C: $S\left(t_s'^{(1)}\right) = S^{\rm SFA}\left(t_s'^{(0)}\right) + G_C\left(\theta_s'^{(0)}, \phi_s'^{(0)}, t_s'^{(0)}\right) + \mathcal{O}\left(\Delta t_s'^{(0)^2}\right)$. However, $t_s'^{(1)}$ will contribute to the pre-exponential factor $P(\theta', \phi', t')$ in the integral.

Below we detail our method and show how it can be used to obtain ionisation amplitudes and ionisation rates using both the time-domain and the frequency domain approaches. The time-domain approach is technically simpler and allows one to consider temporal dynamics of ionisation, including time evolution of electron momentum distributions [19] and ionisation rates.

The paper is organized as follows. Section II introduces basic equations. Section III develops the time-domain approach. Section IV discusses the physical picture arising from

the theory developed in sections II−III. In section IV, we describe modifications of the ionisation dynamics due to the Coulomb effects. These include (i) Coulomb corrections to ionisation times, (ii) initial conditions for electron continuum dynamics and calibration of the attoclock in the angular streaking method, (iii) Coulomb corrections to the "tunnelling angle", including the Coulomb corrections to the ratio of ionisation rates from p^- and p^+ orbitals obtained for the short range potentials in [8]. Section V concludes the work. Appendix A presents additional calculations related to the boundary matching. Appendix B develops the frequency-domain approach, pioneered in the PPT work for the short-range potentials. This approach requires more involved algebra but allows most straightforward connection to the PPT results. Appendix C extends the time domain method in section III to include subcycle dynamics. Appendix D−E present miscellaneous calculations.

II. BASIC EQUATIONS

Following [10], we introduce the Bloch operator $\hat{L}^{\pm}(a)$ to split the configuration space into the inner and outer regions. Parameter a represents the radius of the R-matrix sphere, the inner region is inside the sphere, the outer region is outside of the sphere. The standard Hamiltonian $\hat{H}$ including both Coulomb $V_C(\mathbf{r})$ and laser-field interaction $V_L(t)$:

$$\hat{H} = \frac{\hat{\mathbf{p}}^2}{2} + V_C(\mathbf{r}) + V_L(t) \tag{1}$$

used in the Schordinger equation:

$$i\frac{\partial\psi(\mathbf{r},t)}{\partial t} = \hat{H}\psi(\mathbf{r},t) \tag{2}$$

$$\psi(\mathbf{r}, t = t_0) = \psi_g(\mathbf{r}) \tag{3}$$

can be modified to

$$i\frac{\partial\psi(\mathbf{r},t)}{\partial t} = \hat{H}_B\psi(\mathbf{r},t) - \hat{L}^{\pm}(a)\psi(\mathbf{r},t) \tag{4}$$

where $\hat{H}_B = \hat{H} + \hat{L}^{\pm}(a)$. Following arguments developed in [10], we can express the solution in the outer region via the solution in the inner region as:

$$|\psi_{\rm out}(t)\rangle = i\int_{t_0}^{t} dt'\,\hat{U}_B(t,t')\hat{L}^{-}(a)|\psi_{\rm in}(t')\rangle \tag{5}$$

where for the outgoing solution, we use $\hat{L}^{-}(a)$ and the governing equation for the evolution operator $\hat{U}_B(t,t')$ is:

$$i\frac{\partial}{\partial t}\hat{U}_B(t,t') = \hat{H}_B(t)\hat{U}_B(t,t'). \tag{6}$$

In our time-domain approach detailed in the next section, we start the analysis from the expression for the ionisation amplitude $a_{\mathbf{p}}(T) = \langle \mathbf{p}|\psi_{\rm out}(T)\rangle$ (see [10] for discussion):

$$a_{\mathbf{p}}(T) = i\int_{t_0}^{T} dt' \int d\mathbf{r}' \int d\mathbf{r}'' \, \langle \mathbf{p}|U_B(T,t')|\mathbf{r}'\rangle\langle \mathbf{r}'|\hat{L}^{-}(a)|\mathbf{r}''\rangle\langle \mathbf{r}''|\psi_{\rm in}(t')\rangle \tag{7}$$

Taking into account the explicit form of Bloch operator in coordinate representation:

$$\langle \mathbf{r}'|\hat{L}^{-}(a)|\mathbf{r}''\rangle = \delta(r-a)\delta(\mathbf{r}'-\mathbf{r}'')\hat{B}, \tag{8}$$

$$\hat{B}\psi\left(\mathbf{r},t\right) = \left(\frac{d}{dr}+\frac{1}{r}\right)\psi\left(\mathbf{r},t\right)\Big|_{r=a} \tag{9}$$

we can rewrite Eq. (7) as follows:

$$a_{\mathbf{p}}(T) = i\int_{t_0}^{T} dt' \int d\mathbf{r}' \, G_B(\mathbf{p},T;\mathbf{r}',t')\delta(r'-a)B(a,\theta',\phi',t') \tag{10}$$

where function $B(a,\theta',\phi',t')$ represents the inner region wavefunction at the partition surface $r'=a$ for all times $t_0 < t' < T$:

$$B(a,\theta,\phi,t') = \left(\frac{d}{dr}+\frac{1}{r}\right)\psi_{\rm in}(\mathbf{r},t')\Big|_{r=a} \tag{11}$$

and $G_B(\mathbf{p},T;\mathbf{r}',t') = \langle \mathbf{p}|\hat{U}_B(T,t')|\mathbf{r}'\rangle$ is the Green's function for modified Hamiltonian $\hat{H}_B$ for propagating from the boundary $r'=a$ instead of the origin. As shown in [10], the error incurred in approximating this exact Green function with the Eikonal-Volkov approximated Green's function $G^{\rm EVA}(\mathbf{p},T;\mathbf{r}',t')$ defined on the EVA states [16]:

$$G^{\rm EVA}(\mathbf{p},T;\mathbf{r}',t') = \frac{1}{(2\pi)^{3/2}}\, e^{-i\mathbf{v}_{\mathbf{p}}(t')\cdot\mathbf{r}' - \frac{i}{2}\int_{t'}^{T} d\tau\, v_{\mathbf{p}}^2(\tau)} e^{i\int_{T}^{t'} U(\mathbf{r}_L(\tau;\mathbf{r}',\mathbf{p},t'))} e^{-iG_{0\mathbf{p}}(\mathbf{r}_L(T;\mathbf{r}',\mathbf{p},t'))} \tag{12}$$

is exponentially small. In the above expression we have defined:

$$\mathbf{r}_L(\tau;\mathbf{r},\mathbf{p},t) = \mathbf{r} + \int_{t}^{\tau} d\zeta\, \mathbf{v}_{\mathbf{p}}(\zeta) \tag{13}$$

the characteristic trajectory along which the Coulomb correction is calculated as a perturbation to the Volkov electron [16] and $\mathbf{v}_{\mathbf{p}}(t) = \mathbf{p} + \mathbf{A}(t)$ is the kinetic momentum.

III. THE TIME-DOMAIN APPROACH

We use Eq. (10) for the ionisation amplitude and Eq. (12) to obtain

$$a_{\mathbf{p}}(T) = \frac{i}{(2\pi)^{3/2}}\int_{t_0}^{T} dt' \int d\mathbf{r}'\, e^{-i\mathbf{v}_{\mathbf{p}}(t')\cdot\mathbf{r}'} e^{iS^{\rm SFA}(\mathbf{p},T;\mathbf{r}',t')} e^{iG_C(\mathbf{p},T;\mathbf{r}',t')}\delta(r'-a)B(a,\theta',\phi',t') \tag{14}$$

with the Coulomb phase term defined as:

$$G_C(\mathbf{r}', t', T) = \int_T^{t'} d\tau\, U(\mathbf{r}_L(\tau; \mathbf{r}', \mathbf{p}, t')) \tag{15}$$

Since the time T of observation is sufficiently far, so that we can consider $T \to \infty$ for all practical purposes, we have made the approximation as in [10], of ignoring the distortions of the phase-front from plane wave: $G_{0\mathbf{p}} \to 0$ [16] in Eq. (12). The SFA phase is given by

$$S^{\mathrm{SFA}}(\mathbf{p}, T; \mathbf{r}', t') = -\frac{1}{2}\int_{t'}^{T} d\tau\, v_{\mathbf{p}}^2(\tau) + \frac{\kappa^2}{2}t' \tag{16}$$

A. Transition through the boundary $r' = a$

Function $B(a, \theta', \phi', t')$ reflects the value of the inner-region wave-function at the boundary $r' = a$. In the inner region the Coulomb field dominates and the effects of the laser field on the inner region wave-function $\psi_{\mathrm{in}}(\mathbf{r}', t')$ can be included in quasistatic approximation. Following [10], the boundary is placed in the asymptotic region $E_0 a/I_p \ll 1 \ll \kappa a$ of the ground state wave-function, where $\kappa = \sqrt{2I_p}$, E_0 is the amplitude of the laser field. In this region the difference between polarised and initial wave-function is of the order of $\sim E_0 a^2/\kappa$ [20]. Thus, for sufficiently weak fields such that $E_0/\kappa^3 \ll 1/a^2\kappa^2$ the inner region wave-function $\psi_{\mathrm{in}}(\mathbf{r}', t')$ can be substituted by the field-free bound state wave-function, without affecting the boundary matching. This approximation was first used in the PPT method [14]. The asymptotic radial part of this wave-function is given by:

$$\varphi_{\kappa\ell}(r') = C_{\kappa\ell}\kappa^{3/2}\frac{e^{-\kappa r'}}{\kappa r'}(\kappa r')^{Q/\kappa} \tag{17}$$

Due to the invariance of the boundary term under addition of a function b_0/r', we can choose b_0 appropriately to get:

$$\begin{aligned} B(a, \theta', \phi', t') &= \left(\frac{d}{dr'} - \frac{b_0 - 1}{r'}\right)\varphi_{\kappa\ell}(r')\Big|_{r'=a} \\ &= -\kappa\varphi_{\kappa\ell}(a) \end{aligned} \tag{18}$$

for $b_0 = Q/\kappa$. Using Eq. (18) and evaluating the Delta function over r':

$$a_{\mathbf{p}}(T) = \frac{i\kappa a^2}{(2\pi)^{3/2}}\int_{t_0}^{T} dt' \int d\Omega'\, e^{-i\mathbf{v}_{\mathbf{p}}(t')\cdot\mathbf{a} - \frac{i}{2}\int_{t'}^{T} d\tau\, v_{\mathbf{p}}^2(\tau)} e^{iG_C(\mathbf{p}, T; \mathbf{a}, t')}\varphi_{\kappa\ell}(a) N_{\ell m} P_\ell^m(\cos\theta') \\ e^{im\phi'} e^{i\kappa^2(t'-t_0)/2} \tag{19}$$

where $N_{\ell m} = \sqrt{\frac{2\ell+1}{4\pi}\frac{(\ell-|m|)!}{(\ell+|m|)!}}$, $\mathbf{a} = a(\sin\theta'\cos\phi'\,\hat{\mathbf{x}} + \sin\theta'\sin\phi'\,\hat{\mathbf{y}} + \cos\theta'\,\hat{\mathbf{z}})$. We use $\mathbf{A}(t) = -A_0(\cos\omega t\,\hat{\mathbf{x}} + \sin\omega t\,\hat{\mathbf{y}})$.

Note that in the outer region, the long-range interaction of the electron with the core is described by the phase term $G_C(\mathbf{p}, T; \mathbf{r}', t')$, and involves integration of Coulomb potential along the electron trajectory in the laser field. The trajectory originates from the point $\mathbf{a}$ on the boundary at the time t' (Eq. 13).

B. Iterative approach to solution of saddle point equations

The calculation of the ionisation amplitude $a_{\mathbf{p}}(T)$ involves integration over all starting points of the trajectory on the sphere and all the times t' of "transition" through the boundary $r' = a$. The integrand of Eq. (19) can be written in the form $P(\theta', \phi', t')e^{iS(\theta',\phi',t')}$, where the prefactor $P(\theta', \phi', t')$ reflects the value of the inner-region wave-function at the boundary $r' = a$, and exponent is given by the electron action. The action $S(\theta', \phi', t')$ consists of two parts: $S = S^{\mathrm{SFA}} + G_C$, where S^{SFA} is the SFA action (Eq. 16), associated with the ionisation dynamics in the short range potential, and G_C (Eq. 15) is the term responsible for the long-range interaction with the core, describing the Coulomb-laser coupling [18].

Due to the large value of the action S for the electron in a strong laser field, the integrals are accumulated in the vicinity of stationary (saddle) points θ'_s, ϕ'_s and t'_s, which satisfy the equations:

$$\frac{\partial S}{\partial \theta'} = 0, \quad \frac{\partial S}{\partial \phi'} = 0, \quad \frac{\partial S}{\partial t'} + a\frac{\partial v_{\mathbf{p}}(t')}{\partial t'} = 0 \tag{20}$$

where the saddle point in time has an additional term $a v_{\mathbf{p}}(t')$, which, as we will show in Appendix B 1, is a result of propagation from a finite boundary, and comes from the exact evaluation of the surface integral.

To solve these equations, we recall that by construction, in the outer region G_C presents a perturbation to S^{SFA} and therefore can only slightly shift the SFA saddle points $\theta_s'^{(0)}$, $\phi_s'^{(0)}$ satisfying the equations:

$$\frac{\partial S^{\mathrm{SFA}}}{\partial \theta'} = 0, \quad \frac{\partial S^{\mathrm{SFA}}}{\partial \phi'} = 0, \quad \frac{\partial S^{\mathrm{SFA}}}{\partial t'} + a\frac{\partial v_{\mathbf{p}}(t')}{\partial t'} = 0 \tag{21}$$

Thus, the saddle points for the total action $S = S^{\mathrm{SFA}} + G_C$ can be written as:

$$\theta'_s = \theta_s'^{(0)} + \Delta\theta'_s, \quad \phi'_s = \phi_s'^{(0)} + \Delta\phi'_s, \quad t'_a = t_a'^{(0)} + \Delta t'_a \tag{22}$$

where $\Delta\theta'_s$, $\Delta\phi'_s$, $\Delta t'_a$ are the small corrections to the SFA saddle points and can be found perturbatively. Subscript "a" in $\Delta t'_a$ indicates that the time $\Delta t'_a$ and the time $t'^{(0)}_a$ are affected by the position of the boundary due to the boundary-dependent term $a\frac{\partial v_{\mathbf{p}}(t')}{\partial t'}$ in Eq. (20) and (21). In the first order of perturbation w.r.t. G_C, all deviations from the SFA saddle point solutions are proportional to G_C: $\Delta\theta'_s \sim \mathcal{O}(G_C)$, $\Delta\phi'_s \sim \mathcal{O}(G_C)$ and $\Delta t'_a \sim \mathcal{O}(G_C)$. In our analysis we shall consistently keep only terms of the order $\sim \mathcal{O}(G_C)$ and therefore, only the SFA saddle points can enter the argument of $G_C(\mathbf{p}, T; \mathbf{a}, t')$ and the SFA action. Indeed using Eq. (21) we obtain:

$$G_C(\mathbf{p}, T; \mathbf{a}, t') = G_C\left(\mathbf{p}, T; \mathbf{r}'^{(0)}_s, t'^{(0)}_a\right) + \mathcal{O}(G_C^2) \tag{23}$$

$$S^{\mathrm{SFA}}(\mathbf{p}, T; \mathbf{a}, t') = S^{\mathrm{SFA}}\left(\mathbf{p}, T; \mathbf{r}'^{(0)}_s, t'^{(0)}_a\right) + \mathcal{O}(G_C^2) \tag{24}$$

However, the corrected saddle point solution for time will contribute to the pre-exponential factor $P(\theta', \phi', t')$, since $\frac{\partial P(\theta', \phi', t')}{\partial t'} \neq 0$. It is straightforward to show that $\theta'^{(0)}_s = \theta_v(t')$ and $\phi'^{(0)}_s = \phi_v(t')$, where $\theta_v(t')$ and $\phi_v(t')$ describe the direction of electron velocity at time t'.

C. Integration over the surface sphere

Because of the large value of the action, only a vicinity of saddle points contributes to the integral. We make Taylor expansion of G_C around points $\theta'^{(0)}_s$, $\phi'^{(0)}_s$, $t'^{(0)}_a$ (only the saddle point in time is affected by the boundary term $av_{\mathbf{p}}(t')$) up to quadratic terms:

$$\begin{aligned} G_C(\mathbf{p}, T; \mathbf{a}, t') &= G_C\left(\mathbf{p}, T; \mathbf{r}'^{(0)}_s, t'^{(0)}_a\right) + \left(\mathbf{a} - \mathbf{r}'^{(0)}_s\right) \cdot \nabla G_C\left(\mathbf{p}, \mathbf{r}'^{(0)}_s, t'^{(0)}_a\right) \\ &+ \left(t' - t'^{(0)}_a\right) \partial_{t'} G_C\left(\mathbf{p}, T; \mathbf{r}'^{(0)}_s, t'^{(0)}_a\right) + \frac{1}{2}\left(t' - t'^{(0)}_a\right)^2 \partial^2_{t'} G_C\left(\mathbf{p}, T; \mathbf{r}'^{(0)}_s, t'^{(0)}_a\right) \end{aligned} \tag{25}$$

The mixed derivative $\nabla\partial_{t'} G_C\left(\mathbf{p}, T; \mathbf{r}'^{(0)}_s, t'^{(0)}_a\right) \propto \mathcal{O}(G_C^2)$ is omitted from Eq. (25), as higher order correction, since it is multiplied to $t' - t'^{(0)}_a \propto \mathcal{O}(G_C)$. The term involving second derivatives w.r.t. spatial coordinates on the surface sphere $\frac{1}{2}\left(\mathbf{a} - \mathbf{r}'^{(0)}_s\right)^2 \Delta G_C\left(\mathbf{p}, T; \mathbf{r}'^{(0)}_s, t'^{(0)}_a\right)$ is equal to zero for Coulomb potential, since $\Delta U(r) = \delta(r)$ and the argument of U in $G_C\left(\mathbf{p}, T; \mathbf{r}'^{(0)}_s, t'^{(0)}_a\right)$ is trajectory starting at the surface and propagating outside of the sphere; this trajectory never reaches the origin. Note that $\nabla G_C = \Delta\mathbf{p}$, where $\Delta\mathbf{p}$ is the shift of canonical momentum due to electron interaction with the long range potential of the core:

$$\Delta\mathbf{p}(t', T) \equiv \nabla G_C = -\int_{t'}^{T} d\tau \, \frac{U'}{\left\|\mathbf{r}' + \int_{t'}^{\tau} d\zeta \, \mathbf{v}_{\mathbf{p}}(\zeta)\right\|} \left[\mathbf{r}' + \int_{t'}^{\tau} d\zeta \, \mathbf{v}_{\mathbf{p}}(\zeta)\right] \tag{26}$$

where U' represents derivative of U w.r.t. its argument. It is convenient to rewrite the time derivative of $G_C(\mathbf{p}, T; \mathbf{a}, t')$ as [16]:

$$\begin{aligned}\partial_{t'} G_C\left(\mathbf{p}, T; \mathbf{r}_s'^{(0)}, t_a'^{(0)}\right) &= -\mathbf{v}_{\mathbf{p}}\left(t_a'^{(0)}\right) \cdot \nabla G_C\left(\mathbf{p}, T; \mathbf{r}_s'^{(0)}, t_a'^{(0)}\right) + U(a) \\ &= -\mathbf{v}_{\mathbf{p}} \cdot \Delta\mathbf{p}\left(t_a'^{(0)}, T\right) + U(a)\end{aligned} \tag{27}$$

Substituting Eq. (25) into the expression for $a_{\mathbf{p}}(T)$, and evaluating the integral over ϕ' and θ' exactly (see Appendix B 1) we obtain:

$$\begin{aligned}a_{\mathbf{p}}(T) = N_{\ell m}(-i)^{\ell}(-1)^m \varphi_{\kappa\ell}(a) \frac{2i\kappa a^2}{\sqrt{2\pi}} e^{iG_C\left(\mathbf{p},T;\mathbf{r}_s'^{(0)},t_a'^{(0)}\right)} \int_{t_0}^{T} dt'\, e^{-\frac{i}{2}\int_{t'}^{T} d\tau\, v_{\mathbf{p}}^2(\tau) + i\kappa^2(t'-t_0)/2} \\ e^{i\left(t'-t_s'^{(0)}\right)\partial_{t'} G_C\left(\mathbf{p},T;\mathbf{r}_s'^{(0)},t_s'^{(0)}\right)} e^{im\phi_v^c(t')} P_{\ell}^m\left(\frac{p_z^c}{v_{\mathbf{p}^c}(t')}\right) j_{\ell}\left(a v_{\mathbf{p}}(t')\right)\end{aligned} \tag{28}$$

where $\phi_v^c(t')$ is the tunnelling angle:

$$\tan\phi_v^c(t') = \frac{p_y - \Delta p_y(t', T) + A_y(t')}{p_x - \Delta p_x(t', T) + A_x(t')} \tag{29}$$

and $\mathbf{p}^c = \mathbf{p} - \Delta\mathbf{p}(t', T)$ is the Coulomb-shifted momentum at time t' corresponding to asymptotic momentum $\mathbf{p}$ registered at the detector at time T:

$$\Delta\mathbf{p}(t', T) = \nabla G_C\left(\mathbf{p}, T; \mathbf{r}_s'^{(0)}, t'\right) \tag{30}$$

Note that the tunnelling angle is complex. It signifies sensitivity of strong-field ionisation to the sense of rotation of the electron in the initial state [8, 21].

D. Integration over time

We are now left with the integral over t'. We will use the saddle point method to evaluate this integral. The saddle point equation for t' is:

$$\frac{\partial S}{\partial t'} = \frac{\partial S^{\mathrm{SFA}}}{\partial t'} + \frac{\partial G_C}{\partial t'} + \left(t' - t_a'^{(0)}\right)\frac{\partial^2 G_C}{\partial t'^2} + a v_{\mathbf{p}}'(t') = 0 \tag{31}$$

where the last term, as discussed in subsection III E, comes from $j_{\ell}\left(a v_{\mathbf{p}}(t')\right)$. To solve this equation, we expand the derivative of the SFA action in Eq. (31) up to quadratic terms w.r.t. $\Delta t_a'^{(0)}$ and take into account that $\partial_{t'} S_a^{\mathrm{SFA}}\left(t_a'^{(0)}\right) = 0$, yielding:

$$\Delta t_a'^{(0)} = -\frac{\partial_{t'} G_C\left(t_a'^{(0)}\right)}{\partial_{t'}^2 S_a^{\mathrm{SFA}}\left(t_a'^{(0)}\right) + \partial_{t'}^2 G_C\left(t_a'^{(0)}\right)} \simeq -\frac{\partial_{t'} G_C\left(t_a'^{(0)}\right)}{\partial_{t'}^2 S_a^{\mathrm{SFA}}\left(t_a'^{(0)}\right)} \simeq -\frac{\partial_{t'} G_C\left(t_a'^{(0)}\right)}{\partial_{t'}^2 S_a^{\mathrm{SFA}}\left(t_s'^{(0)}\right)} \tag{32}$$

Here we have used that $t_s'^{(0)} - t_a'^{(0)} = -ia/\kappa \ll t_s'^{(0)}$ [10]. We have omitted terms of order of G_C in the denominator in the last term in Eq. (32), since the terms of the first order of G_C are already included in the denominator. Taking into account Eq. (27) and

$$\partial_{t'}^2 S_a^{\mathrm{SFA}}\left(t_s'^{(0)}\right) = -\mathbf{E}\left(t_s'^{(0)}\right)\cdot\mathbf{v}_{\mathbf{p}}\left(t_s'^{(0)}\right) \tag{33}$$

we obtain for the time:

$$\Delta t_a'^{(0)} = \frac{-\mathbf{v}_{\mathbf{p}}\left(t_s'^{(0)}\right)\cdot\Delta\mathbf{p}\left(t_a'^{(0)},T\right)+U(a)}{\mathbf{E}\left(t_s'^{(0)}\right)\cdot\mathbf{v}_{\mathbf{p}}\left(t_s'^{(0)}\right)} \tag{34}$$

Eq. (23) and (24) suggest that Coulomb corrections to the ionisation time do not affect the exponent of the ionisation amplitude, but they contribute to the prefactor, further modifying the tunnelling angle:

$$\tan\phi_v^c\left(t_a'^{(0)}+\Delta t_a'^{(0)}\right) = \frac{p_y-\Delta p_y\left(t_a'^{(0)}+\Delta t_a'^{(0)},T\right)+A_y\left(t_a'^{(0)}+\Delta t_a'^{(0)}\right)}{p_x-\Delta p_x\left(t_a'^{(0)}+\Delta t_a'^{(0)},T\right)+A_x\left(t_a'^{(0)}+\Delta t_a'^{(0)}\right)} \tag{35}$$

Up to first order terms w.r.t. to G_C, $a_{\mathbf{p}}(T)$ is:

$$\begin{aligned} a_{\mathbf{p}}(T) = i\kappa a^2\varphi_{\kappa\ell}(a)N_{\ell m}\sqrt{\frac{1}{S''\left(t_a'^{(1)}\right)}}e^{-\frac{i}{2}\int_{t_s'^{(0)}}^{T}d\tau\, v_{\mathbf{p}}^2(\tau)+i\kappa^2 t_s'^{(0)}/2+iG_C\left(\mathbf{p},T;\mathbf{r}_s'^{(0)},t_a'^{(0)}\right)} \\ e^{im\phi_v^c\left(t_a'^{(1)}\right)}P_\ell^m\left(\frac{p_z^c}{v_{\mathbf{p}^c}\left(t_a'^{(1)}\right)}\right)j_\ell\left(av_{\mathbf{p}}\left(t_a'^{(1)}\right)\right) \end{aligned} \tag{36}$$

E. Boundary matching

We now consider the elimination of boundary-dependence in the results for transition amplitude. In the long pulse, due to cylindrical symmetry of the problem, the result does not depend on position of the detector in the polarisation plane x, y. Thus, without the loss of generality we will consider electron registered at the detector placed in the positive direction of x-axis, i.e. the electron momentum at the detector $p_y = 0$.

1. *Complex momentum* $\Delta\mathbf{p}\left(t_a'^{(0)}, T\right)$ *at the boundary*

To perform boundary matching in Eq. (34) and Eq. (35), we need to evaluate the momentum $\Delta\mathbf{p}\left(t_a'^{(0)}, T\right)$ at the boundary:

$$\Delta\mathbf{p}\left(t_a'^{(0)}, T\right) = -\int_{t_a'^{(0)}}^{T} d\tau\, \nabla U\left(\mathbf{r}_s'^{(0)} + \int_{t_a'^{(0)}}^{\tau} d\zeta\, \mathbf{v}_{\mathbf{p}}(\zeta)\right) \tag{37}$$

Note that $\Delta\mathbf{p}\left(t_a'^{(0)}, T\right)$ is a function of final momentum $\mathbf{p}$. In this section we consider only $\mathbf{p} = \mathbf{p}_{\rm opt}$, corresponding to the momentum at which the probability is maximal, since it is sufficient to calculate the ionisation rates. The photoelectron spectra will be considered in our subsequent publication [19]. In the polarisation plane the optimal momentum $\mathbf{p}_{\rm opt} = (p_{\rm opt}\cos\phi_p, p_{\rm opt}\sin\phi_p)$ is given by radial momentum

$$p_{\rm opt} = A_0\sqrt{1+\gamma^2}\sqrt{\frac{1-\zeta_0}{1+\zeta_0}} \tag{38}$$

for any angle ϕ_p. The parameter $0 \le \zeta_0 \le 1$ satisfies the equation $\sqrt{\frac{\zeta_0^2+\gamma^2}{1+\gamma^2}} = \tanh\frac{1}{1-\zeta_0}\sqrt{\frac{\zeta_0^2+\gamma^2}{1+\gamma^2}}$ [8, 14, 21]. Note that $\zeta_0 \simeq \gamma^2/3$ for $\gamma \ll 1$, and $\zeta_0 \simeq 1 - 1/\ln\gamma$ for $\gamma \gg 1$ [14]. An alternative expression for $p_{\rm opt}$ is

$$p_{\rm opt} = A_0\frac{\sinh\omega\tau_i'^{(0)}}{\omega\tau_i'^{(0)}} \tag{39}$$

where $\tau_i'^{(0)} = \Im[t_s'^{(0)}]$, is the imaginary part of the saddle point solution for time, also known as the "tunnelling time". The advantage of the second expression is that it provides a compact connection between the optimal momentum and the tunnelling time, however, one has to keep in mind that in circular field $\tau_i'^{(0)}$ depends on final radial momentum p [8, 14, 21]:

$$\omega\tau_i'^{(0)} = \cosh^{-1}\eta, \quad \eta(\mathbf{p}) = \frac{A_0}{2p_\rho}\left[\left(\frac{p}{A_0}\right)^2 + \gamma^2 + 1\right] \tag{40}$$

and thus, in Eq. (39), $\tau_i'^{(0)}$ depends on $p_{\rm opt}$ itself.

Since the time $t_a'^{(0)}$ is complex, the momentum $\Delta\mathbf{p}\left(t_a'^{(0)}, T\right)$ will also be complex:

$$\Delta p_y\left(t_a'^{(0)}, T\right) = \Delta p_y'(a) + i\Delta p_y''(a) \tag{41}$$

$$\Delta p_x\left(t_a'^{(0)}, T\right) = \Delta p_x'(a) + i\Delta p_x''(a) \tag{42}$$

After some algebra (see Appendix A 1) we obtain:

$$\Delta p_y''(a) \simeq \mathcal{O}\left(\frac{1}{\kappa a}\right) \to 0 \tag{43}$$

$$\Delta p_x'(a) = \Delta p_x', \quad \Delta p_y'(a) = \Delta p_y' \tag{44}$$

$$\Delta p_x''(a) = \Delta p_x'' + \mathcal{O}\left(\frac{1}{\kappa a}\right) \tag{45}$$

where the boundary independent momentum is

$$\Delta \mathbf{p}' = -\int_{\Re[t_s'^{(0)}]}^{T} d\tau\, \nabla U \left(\mathbf{r}_e'^{(0)} + \int_{\Re[t_s'^{(0)}]}^{\tau} d\zeta\, \mathbf{v}_{\mathbf{p}_{\rm opt}}(\zeta)\right) \tag{46}$$

and the coordinate $\mathbf{r}_e'^{(0)}$, known as the coordinate of exit from the tunnelling barrier, is defined as

$$\mathbf{r}_e'^{(0)} = \int_{t_s'^{(0)}}^{\Re[t_s'^{(0)}]} d\zeta\, \mathbf{v}_{\mathbf{p}_{\rm opt}}(\zeta) \tag{47}$$

Finally (Appendix A 1)

$$\Delta p_x'' \equiv 0 \tag{48}$$

2. Boundary matching for $\Delta t_a'^{(0)}$ in Eq. (34) and for the tunnelling angle $\tan\phi_v^c \left(t_a'^{(0)} + \Delta t_a'^{(0)}\right)$ in Eq. (58)

Substituting Eqs. (43), (44), (45), (46), (48) for $\Delta\mathbf{p}\left(t_a'^{(0)}, T\right)$ from the previous section into Eq. (34) and taking into account that in our geometry

$$E_y\left(t_s'^{(0)}\right) = E_y', \quad E_y' = E_0 \cosh \omega \tau_i'^{(0)} \tag{49}$$

$$E_x\left(t_s'^{(0)}\right) = iE_x'', \quad E_x'' = -E_0 \sinh \omega \tau_i'^{(0)} \tag{50}$$

$$v_y\left(t_s'^{(0)}\right) = iv_y'', \quad v_y'' = -A_0 \sinh \omega \tau_i'^{(0)} \tag{51}$$

$$v_x\left(t_s'^{(0)}\right) = v_x', \quad v_x' = p_{\rm opt} - A_0 \cosh \omega \tau_i'^{(0)} = \frac{a_0}{\tau_i'^{(0)}} \left(\sinh \omega \tau_i'^{(0)} - \omega\tau \cosh \omega \tau_i'^{(0)}\right) \tag{52}$$

where $a_0 = E_0/\omega^2$ is the electron oscillation amplitude, yielding

$$\mathbf{E}\left(t_s'^{(0)}\right) \cdot \mathbf{v}_{\mathbf{p}_{\rm opt}}\left(t_s'^{(0)}\right) = ip_{\rm opt} E_0 \sinh \omega \tau_i'^{(0)} = iv_y'' p_{\rm opt} \omega \tag{53}$$

we obtain:

$$\Im[\Delta t_a'^{(0)}] = \frac{\Delta p_x' v_x'/v_y'' - U(a)/v_y''}{p_{\rm opt}\omega} \tag{54}$$

Since $U(a)/v_y'' \simeq \Delta p_y'' \simeq \mathcal{O}\left(\frac{1}{\kappa a}\right) \to 0$ (see Appendix A 1), $\Delta p_x'' = 0$ we obtain boundary-independent correction to real ionisation time $\Re[\Delta t_s'^{(0)}] = \Re[\Delta t_a'^{(0)}]$ and imaginary ionisation time $\Im[\Delta t_s'^{(0)}] = \Im[\Delta t_a'^{(0)}]$:

$$\Im[\Delta t_s'^{(0)}] = \frac{\Delta p_x' v_x'}{v_y'' p_{\rm opt}\omega} = -\frac{\Delta p_x'}{E_0}\frac{\sinh\omega\tau_i'^{(0)} - \omega\tau\cosh\omega\tau_i'^{(0)}}{\sinh^2\omega\tau_i'^{(0)}} \tag{55}$$

$$\Re[\Delta t_s'^{(0)}] = -\frac{\Delta p_y'}{p_{\rm opt}\omega} = -\frac{\Delta p_y'}{E_0}\frac{\omega\tau_i'^{(0)}}{\sinh\omega\tau_i'^{(0)}} \tag{56}$$

where the subscript "s" denotes that the results for corrections to SFA saddle point $t_a'^{(0)}$ are now independent of the boundary $r' = a$. Thus we can write the saddle point as:

$$t_s'^{(1)} = t_s'^{(0)} + \Delta t_s'^{(0)} \tag{57}$$

Matching for the tunnelling angle is now trivial, since all variables entering Eq. (35) are now proved to be boundary-independent:

$$\tan\phi_v^c\left(t_a'^{(0)} + \Delta t_a'^{(0)}\right) = \frac{v_y\left(t_s'^{(0)}\right) - \Delta p_y - \Delta t_s'^{(0)} E_y}{v_x\left(t_s'^{(0)}\right) - \Delta p_x - \Delta t_s'^{(0)} E_x} \tag{58}$$

3. Boundary matching of remaining terms in Eq. (36)

We first establish the connection (in Appendix A 2):

$$j_\ell\left(a v_{\mathbf{p}^c}\left(t_a'^{(1)}\right)\right) e^{-i\mathbf{r}_s'^{(0)}\cdot\Delta\mathbf{p}} = j_\ell\left(a v_{\mathbf{p}}\left(t_s'^{(0)}\right)\right) \tag{59}$$

Next, we consider matching of the EVA phase to the bound wave-function. We follow the approach used in [10] for linearly polarised field.

$$B(a) = \kappa a^2 \varphi_{\kappa\ell}(a) e^{iG_C\left(\mathbf{r}_s'^{(0)}, t_a'^{(0)}, T\right)} j_\ell\left(a v_{\mathbf{p}}\left(t_s'^{(0)}\right)\right) \tag{60}$$

The asymptotic bounded wavefunction in a Coulomb potential is:

$$\varphi_{\kappa\ell}(r) = C_{\kappa l}\kappa^{3/2}\frac{e^{-\kappa r}}{\kappa r}(\kappa r)^{Q/\kappa} \tag{61}$$

Furthermore, at $r' = a$, we can write $(\kappa a)^{Q/\kappa}$ as

$$(\kappa a)^{Q/\kappa} = e^{Q/\kappa\int_{1/\kappa}^{a}\frac{d\chi}{\chi}} = e^{-i\int_{t_\kappa'^{(0)}}^{t_a'^{(0)}} d\tau\, U\left(\int_{t_s'^{(0)}}^{\tau} d\zeta\, i\kappa\right)} = e^{-i\int_{t_\kappa'^{(0)}}^{t_a'^{(0)}} d\tau\, U\left(\int_{t_s'^{(0)}}^{\tau} d\zeta\, \mathbf{v}(\zeta)\right)} \tag{62}$$

where $t_\kappa'^{(0)} = t_s'^{(0)} - i/\kappa^2$ and $t_a'^{(0)} = t_s'^{(0)} - ia/\kappa$. The second equality follows from the fact that between $t_\kappa'^{(0)}$ and $t_a'^{(0)}$, the velocity of the electron remains almost constant, while the third equality holds because finally we will be using the modulus of the vector and under the approximation:

$$\left\| \int_{t_s'^{(0)}}^{\tau} d\zeta\, \mathbf{v}(\zeta) \right\| \approx \|\mathbf{v}(t_s'^{(0)})\| \left(\tau - t_s'^{(0)}\right) = i\kappa \left(\tau - t_s'^{(0)}\right) = \int_{t_s'^{(0)}}^{\tau} d\zeta\, i\kappa \tag{63}$$

The term given by Eq. (62) can now be matched with the Coulomb phase term $G_C\left(\mathbf{p}, T; \mathbf{r}_s'^{(0)}, t_a'^{(0)}\right)$:

$$G_C\left(\mathbf{r}_s'^{(0)}, t_a'^{(0)}, T\right) = \int_T^{t_a'^{(0)}} d\tau\, U\left(\mathbf{r}_s'^{(0)} + \int_{t_a'^{(0)}}^{\tau} d\zeta\, \mathbf{v}_{\mathbf{p}}(\zeta)\right) = \int_T^{t_a'^{(0)}} d\tau\, U\left(\int_{t_s'^{(0)}}^{\tau} d\zeta\, \mathbf{v}_{\mathbf{p}}(\zeta)\right) \tag{64}$$

to yield after using the large argument approximation for $j_\ell\left(a v_{\mathbf{p}}\left(t_s'^{(0)}\right)\right)$:

$$\begin{aligned} B(a) &= -iC_{\kappa l}\sqrt{\kappa} e^{-\kappa a} e^{-i\int_{t_\kappa'^{(0)}}^{t_a'^{(0)}} d\tau\, U\left(\int_{t_s'^{(0)}}^{\tau} d\zeta\, \mathbf{v}_{\mathbf{p}}(\zeta)\right)} e^{i\int_T^{t_a'^{(0)}} U\left(\int_{t_s'^{(0)}}^{\tau} d\zeta\, \mathbf{v}_{\mathbf{p}}(\zeta)\right)} \\ &\left(e^{-\kappa a - i(\ell+1)\pi/2} + e^{\kappa a + i(\ell+1)\pi/2}\right) \\ &= i^\ell C_{\kappa l}\sqrt{\kappa} e^{i\int_T^{t_\kappa'^{(0)}} d\tau\, U\left(\int_{t_s'^{(0)}}^{\tau} d\zeta\, \mathbf{v}(\zeta)\right)} \left(1 + (-1)^{\ell+1} e^{-2\kappa a}\right) \end{aligned} \tag{65}$$

which ensures boundary matching for all transition rates/amplitudes.

After boundary matching the final expression for the ionisation amplitude is independent of a:

$$\begin{aligned} a_{\mathbf{p}}(T) = (-1)^m C_{\kappa\ell} N_{\ell m} &\sqrt{\frac{\kappa}{S''\left(t_s'^{(1)}\right)}} e^{-\frac{i}{2}\int_{t_s'^{(0)}}^{T} d\tau\, v_{\mathbf{p}}^2(\tau) + i\frac{\kappa^2}{2} t_s'^{(0)}} e^{-i\int_{t_\kappa'^{(0)}}^{T} d\tau\, U\left(\int_{t_s'^{(0)}}^{\tau} d\zeta\, \mathbf{v}_{\mathbf{p}}(\zeta)\right)} \\ &P_\ell^m\left(\frac{p_z^c}{v_{\mathbf{p}^c}\left(t_s'^{(1)}\right)}\right) e^{im\phi_v^c\left(t_s'^{(1)}\right)} \end{aligned} \tag{66}$$

Here $t_s'^{(1)}$ is given by Eq. (57). Eq. (66) corresponds to "single" ionisation event (ionisation amplitude formed after one laser cycle), since only one saddle point is included.

F. Ionisation rate

To calculate the ionisation rate we integrate the ionisation amplitude (corresponding to single ionisation event) over all momenta using the saddle point method and divide by period of the laser field:

$$w = \frac{\omega}{2\pi} \int d\mathbf{p}\, |a_{\mathbf{p}}(T)|^2 \tag{67}$$

In Appendix B 4, we evaluate this integral exactly, but consider here the rate around the optimal momentum. As it follows from Eq. (66), the ionisation amplitude $a_{\mathbf{p}}(T)$ can be written in the form: $a_{\mathbf{p}}(T) = P_{\mathbf{p}} e^{iF_{\mathbf{p}}}$ and the integral Eq. (67) can be calculated using saddle point method.

The saddle point equation

$$\nabla_{\mathbf{p}} 2\Im[F_{\mathbf{p}}] = 2\nabla_{\mathbf{p}} \Im[S^{\mathrm{SFA}}_{\mathbf{p}}] + 2\nabla_{\mathbf{p}} \left[\Im[F_{\mathbf{p}}] - \Im[S^{\mathrm{SFA}}_{\mathbf{p}}]\right] = 0 \tag{68}$$

can again be solved iteratively, since the second term is small by construction. The optimal momentum in SFA solves the equation:

$$2\nabla_{\mathbf{p}} \Im[S^{\mathrm{SFA}}_{\mathbf{p}}] = 0 \tag{69}$$

and is given by Eqs. (38), (39) Since the correction to p_{opt} are obtained from the Eq. (68), they will contribute to the ionisation rate in the second order w.r.t. G_C. We keep only terms of the first order w.r.t. G_C and therefore these corrections are irrelevant and the saddle point for the momentum integral in the ionisation rate is given by the optimal momentum Eq. (38). We neglect here small corrections arising from substituting the pre-exponential factor $S''_{\mathbf{p}}\left(t_s'^{(1)}\right)$ by $S''_{\mathbf{p}}\left(t_s'^{(0)}\right)$ in Eq. (66). Finally, using saddle point method for radial integral and taking into account that integration over ϕ_p yields 2π we obtain the expression for the ionisation rate:

$$\begin{aligned} w_{\mathrm{opt}} = |C_{\kappa\ell}|^2 |N_{\ell m}|^2 \frac{\gamma}{\sqrt{\eta^2-1}} \sqrt{\frac{\pi}{\Im[S''(p_{\rho,\mathrm{opt}})]}} e^{-\frac{4n_0}{1-\zeta_0^2}\sqrt{\frac{\zeta_0^2+\gamma^2}{1+\gamma^2}}} e^{2W_{C1}+2W_{C2}} \\ \left| P_\ell^m\left(\frac{-\Delta k_z}{v_{\mathbf{p}^c}\left(t_s'^{(1)}\right)}\right)\right|^2 e^{-2m\Im\left[\phi_v^c\left(t_s'^{(1)}\right)\right]} \end{aligned} \tag{70}$$

where

$$\Im[S''(p_{\mathrm{opt}})] = \frac{2\zeta_0^2 + \gamma^2(1+\zeta_0^2)}{\omega(1-\zeta_0)\sqrt{(\zeta_0^2+\gamma^2)(1+\gamma^2)}} \tag{71}$$

$$W_{C1} = -\int_0^{\tau_\kappa'^{(0)}} d\tau\, \Re\left[U\left(\int_{t_s'^{(0)}}^{\tau} d\zeta\, \mathbf{v}_{\mathbf{p}}(\zeta)\right)\right] \tag{72}$$

$$W_{C2} = \int_{t_i'^{(0)}}^{T} d\tau \Im\left[U\left(\int_{t_s'^{(0)}}^{\tau} d\zeta\, \mathbf{v}_{\mathbf{p}}(\zeta)\right)\right] \tag{73}$$

W_{C1} is well-known adiabatic Coulomb correction, evaluated under the barrier along the optimal trajectory [14, 15]. Analysis of Eq. (70) shows that non-adiabatic Coulomb effects

modify the ionisation dynamics in several ways. New effects arising from our analysis include: modification of (i) ionisation times, (ii) initial conditions for electron continuum dynamics, (iii) the "tunnelling angle". We discuss these Coulomb effects in detail in the next section. We show that Coulomb effects modify (i) calibration of the attoclock in the angular streaking method, and (ii) the ratio of ionisation rates from p^- and p^+ orbitals obtained for short range potentials in [8]. The photoelectron spectra will be considered in our subsequent publication [19], where we will include the effects of W_{C2}, the result of interaction of long-range potential with the electron in the continuum.

IV. PHYSICAL PICTURE OF IONISATION IN LONG RANGE POTENTIALS

In circularly polarised fields, the electron liberated at different times will be "directed" by the laser field into different angles. This idea is called 'angular streaking' and the corresponding "time-to-angle" mapping is unique for nearly single-cycle pulses with stable carrier-envelope phase, underlying the idea of the atto-clock [1–4]. The angular streaking principle makes single and double ionisation in circularly polarised strong laser fields a sensitive probe of the attosecond dynamics [1–6].

However, reconstruction of this dynamics requires the calibration of the attoclock, i.e. establishing the mapping between the direction of the laser polarisation vector at the time of ionisation and the direction of the electron momentum at the detector. When one strives to achieve the accuracy of, say, 10 attoseconds, using 800 nm carrier as a clock, one needs to know this mapping with accuracy of about one degree.

Simple analytical calibration can be made if one neglects the electron interaction with the the long-range core potential during and after ionisation. For short range potentials the mapping is illustrated in Fig. 1. For the laser field defined as:

$$\mathbf{E}(t) = E_0(-\sin(\omega t)\,\hat{\mathbf{x}} + \cos(\omega t)\,\hat{\mathbf{y}}) \tag{74}$$

the connection between the real part of the ionisation time and the observation angle is [14, 21]:

$$\omega t_i'^{(0)} = \omega \Re[t_s'^{(0)}] = \phi_p + 2\pi(r-1),\ r \in \mathbb{N} \tag{75}$$

The detector placed at positive direction of x-axis will detect the electron liberated at $t_i'^{(0)} = 0$, i.e. when the laser field $\mathbf{E}(t) = E_0\hat{\mathbf{y}}$ is pointing towards the positive direction of

y-axis. The electron exits the barrier in the negative direction of y-axis, corresponding to the angle $-\pi/2$. The velocity at the exit $v_y\left(t_i'^{(0)}\right) = 0$, $v_x\left(t_i'^{(0)}\right) = p_{\rm opt} - A_0$, and $v_x\left(t_i'^{(0)}\right)$ tends to zero in tunnelling limit ($\gamma \ll 1$): $v_x\left(t_i'^{(0)}\right) = \sqrt{2I_p}\gamma/6$. Thus, the angle between the direction of the field at the moment of ionisation and the electron momentum at the detector is $\pi/2$.

How this mapping is affected when the interaction with the long-range core potential is taken into account?

A. Coulomb correction to the ionisation time, initial electron velocity and the calibration of the attoclock

Even in the tunnelling limit, our analysis shows that due to the effects of the long-range potential the electron has non-zero velocity ($-\Delta p_y$) in the negative direction of the y-axis when the field is pointing in the positive y-direction, i.e. at $t = 0$ in our notations.

This is by no means surprising and the corresponding velocity has a very simple explanation: it is required to overcome the attraction of the Coulomb potential, which the electron will experience all the way towards the detector. Had the electron been born with zero velocity in long range potential, it would have never reached the detector placed in positive direction of x-axis. One expects the same result within the adiabatic tunnelling picture. The question is: is the magnitude of Δp_y consistent with the adiabatic ionisation model, which would suggest that the electron was liberated slightly before $t = 0$ but with zero velocity?

To answer this question, we need to analyse the changes in the ionisation time due to the effects of the long-range potential. The corrections to ionisation times associated with electron interaction with the long-range potential are given by Eqs. (55) and (56). The shift of the saddle point in time $\Re[\Delta t_s'^{(0)}]$ corresponds to the shift in the direction of the force of the electric field $-\mathbf{E}(t)$ from $-\pi/2$ to $-\pi/2 + \omega\Re[\Delta t_s'^{(0)}]$.

Let us first discuss the initial conditions for the electron continuum dynamics in the tunnelling limit $\gamma \ll 1$. In this limit, the momentum shift is accumulated along the electron trajectory:

$$\mathbf{r}^{\rm tun}(t) = \int_{t_s'^{(0)}}^{t} d\zeta \mathbf{v}(\zeta) = -\left[i\kappa\left(t - t_s'^{(0)}\right) + \frac{E_0}{2}\left(t - t_s'^{(0)}\right)^2\right]\hat{\mathbf{y}} \tag{76}$$

The tunnelling trajectory along y-axis can be further rewritten as: $y^{\rm tun}(t) = -I_p/E_0 -$

$\frac{1}{2}E_0\left(t-t_i'^{(0)}\right)^2$. Hence, we are only left with the real part where $y^{\rm tun}\left(t_i'^{(0)}\right)=-I_p/E_0$ is the coordinate of the exit point in the tunnelling limit. Taking into account that $U=-Q/(-y)$, $\nabla U=-Q\hat{\mathbf{y}}/y^2$ and substituting this trajectory into the expression for $\Delta\mathbf{p}$, Eq. (46), we obtain:

$$\Re[\Delta p_y]=-Q\int_{t_i'^{(0)}}^{T}\frac{d\tau}{(y^{\rm tun})^2}=-\frac{0.78\sqrt{2}}{I_p^{3/2}}QE_0, \tag{77}$$

It is easy to see that Eq. (56) in the tunnelling limit yields $\Re[\Delta t_s'^{(0)}]=-\Delta p_y'/E_0$, thus we obtain from Eq. (77):

$$\Delta t_i'^{(0)}=-\frac{0.78Q\sqrt{2}}{I_p^{3/2}}\approx -I_p^{3/2} \tag{78}$$

From Eq. (78), we find that the correction to the ionisation time $\Re[\Delta t_s'^{(0)}]$ is negative, the electron is born before $\mathbf{E}(t)$ points down, and the Coulomb corrected angle $-\pi/2+\omega\Re[\Delta t_s'^{(0)}]$ has a larger negative value. At this (earlier) ionisation time the electron velocity is smaller than at $t_i'^{(0)}$ and in the tunnelling limit:

$$v_x=p_{\rm opt}-A_0\cos\left(\omega t_i'^{(0)}+\omega\Re[\Delta t_s'^{(0)}]\right)-\Delta p_x'\approx p_{\rm opt}-A_0+\mathcal{O}(G_C^2)\approx\gamma\sqrt{2I_p}/6+\mathcal{O}(G_C^2) \tag{79}$$

$$v_y=-\Delta p_y-A_0\sin\left(\omega t_i'^{(0)}+\omega\Re[\Delta t_s'^{(0)}]\right)=-\Delta p_y-A_0\omega\Re[\Delta t_s'^{(0)}]\approx 0+\mathcal{O}(G_C^2) \tag{80}$$

Thus, in the tunnelling limit $\gamma\to 0$, the electron velocity indeed tends to zero at the exit from the barrier. The effect of Coulomb potential is reduced to the modification of the angle between the direction of the laser field at the moment of exit $\mathbf{E}\left(t_i'^{(0)}\right)$ and the direction of final electron momentum $\mathbf{p}$, registered at the detector. For short range potentials this angle is $\pi/2$, for long range potential this angle is larger; in tunnelling limit it is $\pi/2+\omega I_p^{-3/2}$, see Fig. 1.

However, most of the experiments are currently performed in the regime of non-adiabatic ionisation, when the Keldysh parameter γ is not that small. In this regime the exit velocities:

$$v_x=p_{\rm opt}-A_0\cos\left(\omega\Re[\Delta t_s'^{(0)}]\right)-\Delta p_x \tag{81}$$

$$v_y=-\Delta p_y-A_0\sin\left(\omega\Re[\Delta t_s'^{(0)}]\right) \tag{82}$$

become significant already for small γ. The longitudinal electron velocity $v_\parallel$ along the direction of the field and the electron transverse velocity $v_\perp$ orthogonal to the field are also

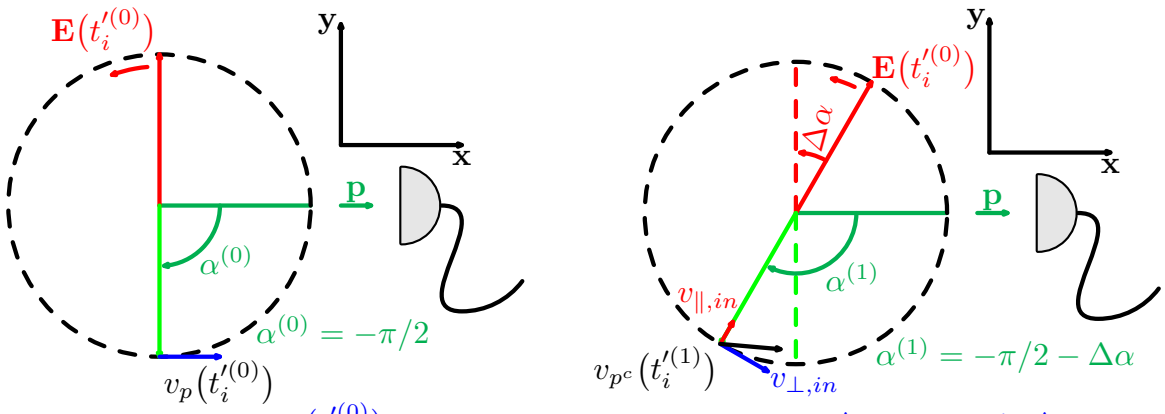

(a)Short Range Potential

(b)Long Range Potential

FIG. 1. Kinematics of electron tunnelling through rotating barrier. Right circularly polarised laser field E creates the tunnelling barrier rotating counter-clockwise. (a) Short range potential: The electron observed at the detector placed along the x-axis, exits the barrier along the negative direction of y-axis at angle $\alpha^{(0)} = -\pi/2$. (b) Long range potential: The electron observed at the detector placed along the x-axis, exits the barrier at the angle $\alpha^{(1)} = -\pi/2 - \Delta\alpha$, $\Delta\alpha = \left|\omega\Delta t_i'^{(0)}\right|$ and $\Delta t_i'^{(0)} < 0$.

non-zero (Fig. 2). The longitudinal and transverse velocities are obtained from Eqs. (81) and (82) ($\Delta\alpha = \left|\omega\Delta t_i'^{(0)}\right|$):

$$v_\perp = v_x\cos(\Delta\alpha) - v_y\sin(\Delta\alpha) \tag{83}$$

$$v_\parallel = v_x\sin(\Delta\alpha) + v_y\cos(\Delta\alpha) \tag{84}$$

Ignoring non-zero initial velocity of the electron will lead to errors in the two-step reconstruction of time delays in angular streaking method.

B. Coulomb correction to the electron "tunnelling angle"

The complex tunnelling angle characterises the direction of the electron velocity at the complex ionisation time $t_s'^{(1)}$: $\tan\phi_v(t_s'^{(1)}) = \frac{v_y(t_s'^{(1)})}{v_x(t_s'^{(1)})}$. The ionisation rate is proportional to the imaginary part of the tunnelling angle $w \propto e^{2m\Im[\phi_v(t_s'^{(1)})]}$, where m is the magnetic quantum number. In case of spherically symmetric initial state (s-state) $m = 0$ and the ionisation rate does not depend on the tunnelling angle, because the electron density in

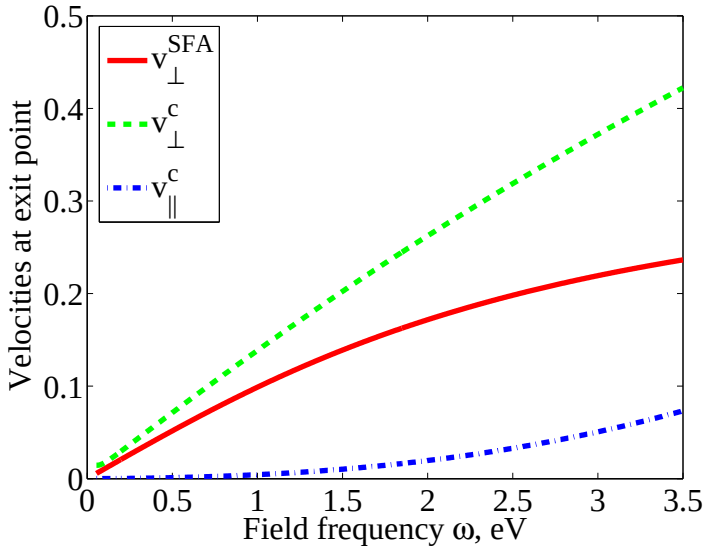

FIG. 2. Initial velocity corresponding to the center of the velocity distribution: $v_\perp$ (green dashed) (Eq. 83) and $v_\parallel$ (blue dot-dashed) (Eq. 84) vs frequency for $E_0 = 3 \times 10^{10}$ V/m ($E_0 = 0.06$ a.u. and $I = 2.6 \times 10^{14}$ W/cm^2) and $I_p = 14$ eV. $v_\perp^{\rm SFA}$ (red) shows the result for short-range potentials (SFA velocity).

the initial state is the same in all directions. For p-states however, the direction of electron tunnelling, defined by the tunnelling angle, becomes important. In particular, it leads to the sensitivity of ionisation to the sense of rotation of the electron in the initial state. For short range potentials this effect was predicted and analysed in [8]. In this section we discuss the non-adiabatic Coulomb corrections to the tunnelling angle and show how the results of [8] are affected by the electron interaction with the long-range core potential.

The tunnelling angle in case of short-range potentials is:

$$\tan\phi_v\left(t_s'^{(0)}\right) = \frac{p_y - A_0\sin\left(\omega t_s'^{(0)}\right)}{p_x - A_0\cos\left(\omega t_s'^{(0)}\right)} \tag{85}$$

The Coulomb potential leads to the two equally important effects: (i) the modification of the complex ionisation time ($t_s'^{(0)} + \Delta t_s'^{(0)}$ in the long-range potential vs. just $t_s'^{(0)}$ in the short range potential), and (ii) the momentum shift due to the deceleration of the electron by the long-range potential of the core (see derivation in subsection III E):

$$\tan\phi_v^c(t_s') = \frac{v_y\left(t_s'^{(0)}\right) - \Delta p_y - \Delta t_s'^{(0)} E_y}{v_x\left(t_s'^{(0)}\right) - \Delta p_x - \Delta t_s'^{(0)} E_x} \tag{86}$$

In this section we focus on the imaginary part of the complex tunnelling angle $\phi_v^c(t'_s) = \tan^{-1}(x+iy)$, since it contributes to the ionisation probability. The imaginary part of $\phi_v^c(t'_s)$ can be cast in the form:

$$\Im[\phi_v^c(t'_s)] = -\frac{1}{4}\ln\left(\left(1-x^2-y^2\right)^2+4x^2\right)+\frac{1}{2}\ln\left((1+y)^2+x^2\right) \tag{87}$$

Note that the real part $x \simeq \mathcal{O}(G_C)$ is of the first order with respect to long-range potential and therefore the x^2 terms have to be omitted. The ratio between ionisation rates for p^- and p^+ orbitals is

$$\frac{w_{p^-}}{w_{p^+}} = \left|\frac{e^{-i2\phi_v^c(t_s'^{(1)})}}{e^{i2\phi_v^c(t_s'^{(1)})}}\right| = e^{4\Im[\phi_v^c(t_s'^{(1)})]} = \left(\frac{1+y}{1-y}\right)^2 \tag{88}$$

$$y = \frac{v''_y - \Im[\Delta t_s'^{(0)}]E'_y}{v'_x - \Delta p'_x + \Im[\Delta t_s'^{(0)}]E''_x} \tag{89}$$

Finally,

$$y = \frac{v''_y + \Delta p'_x v'_x/[p_{\rm opt}\tanh\omega\tau]}{v'_x - \Delta p'_x + \Delta p'_x v'_x/p_{\rm opt}} \tag{90}$$

Fig. 3 shows how the non-adiabatic Coulomb effects change the ratio between the ionisation rates for the p^+ and p^- orbitals. Modifications come solely from the alteration of the tunnelling angle. The non-adiabatic Coulomb corrections (W_{C1} and W_{C2}) do not contribute to the ratio of the ionisation rates, as has been also noted in [8]. The decrease in the p^-/p^+ ratio at high frequencies in long-range potentials is consistent with the opposite propensity rules in one photon ionisation, where p^+ is preferred over p^- for right circularly polarised fields.

V. CONCLUSION

We have evaluated strong field ionisation rates and amplitudes for circular fields taking into account non-adiabatic barrier dynamics of a Coulomb potential using the recently developed ARM technique. The ionisation rates for atoms in arbitrary potentials in circular fields for long range potentials have been derived rigorously, extending the work of [8, 10] and [14, 22]. Along with the Eikonal-Volkov approximation to the free electron state, the ARM approach allows for accurate and rigorous analysis of ionisation in strong fields, consistently including the Coulomb effects both during and after ionisation. It should be noted that in the current implementation of the ARM we have included Coulomb effects in first

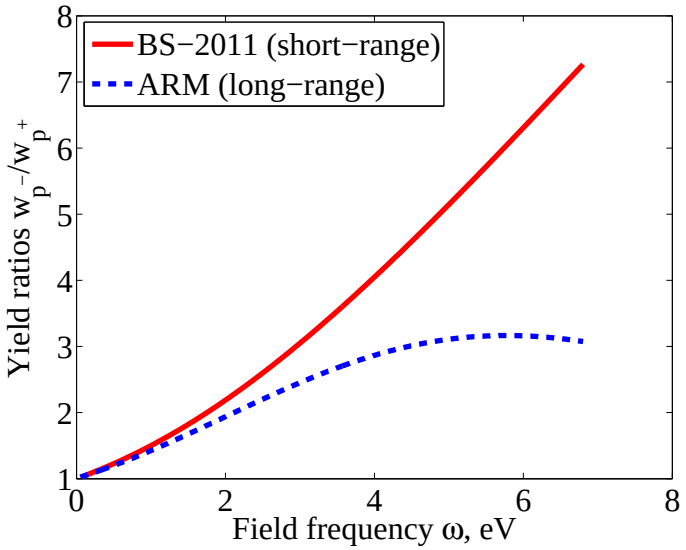

FIG. 3. The ratio of ionisation rates from p^- and p^+ orbitals for Ne atom ($I_p = 21.5645$ eV) and $E_0 = 7.7 \times 10^{10}$ V/m ($E_0 = 0.15$ a.u. and $I = 1.6 \times 10^{15}$ W/cm^2): w_{p^-}/w_{p^+} for right circularly polarised field: short range potential (red) [8], and long range potential (blue dashed).

order perturbation to the action. It limits the applicability of current implementation to the region of moderate γ. The simplest "post-mortem" validity check can be performed by computing $\Delta\mathbf{p}'$ (Eq. 46) and comparing it to the SFA velocities. The momentum shifts $\Delta\mathbf{p}'$ should not exceed the SFA velocities.

ACKNOWLEDGMENTS

O.S. and J.K. acknowledge support from Marie Curie ITN CORINF. We thank M. Ivanov for many useful discussions and encouragement throughout the work.

Appendix A: Supplementary information for boundary matching

1. Complex momentum shifts at the boundary

The goal of this section is to calculate momentum shift at the matching point a:

$$\Delta\mathbf{p}(a) = -\int_{t_a'^{(0)}}^{T} d\tau\, \nabla U \left(\mathbf{r}_s'^{(0)} + \int_{t_a'^{(0)}}^{\tau} d\zeta\, \mathbf{v}_\mathbf{p}(\zeta) \right) \tag{A1}$$

and show that it does not depend on the position of the boundary under the matching conditions. We first split the integral into two parts:

$$\Delta\mathbf{p}(a) = -\int_{t_a'^{(0)}}^{\Re[t_s'^{(0)}]} d\tau\, \nabla U\left(\mathbf{r}_s'^{(0)} + \int_{t_a'^{(0)}}^{\tau} d\zeta\, \mathbf{v}_\mathbf{p}(\zeta)\right) - \int_{\Re[t_s'^{(0)}]}^{T} d\tau\, \nabla U\left(\mathbf{r}_s'^{(0)} + \int_{t_a'^{(0)}}^{\tau} d\zeta\, \mathbf{v}_\mathbf{p}(\zeta)\right) \tag{A2}$$

Physically, these two parts can be interpreted as accumulated before:

$$\Delta\mathbf{p}^{(1)}(a) = \int_{t_a'^{(0)}}^{\Re[t_s'^{(0)}]} d\tau\, \nabla U\left(\mathbf{r}_s'^{(0)} + \int_{t_a'^{(0)}}^{\tau} d\zeta\, \mathbf{v}_\mathbf{p}(\zeta)\right) \tag{A3}$$

and after:

$$\Delta\mathbf{p}^{(2)}(a) = \int_{\Re[t_s'^{(0)}]}^{T} d\tau\, \nabla U\left(\mathbf{r}_s'^{(0)} + \int_{t_a'^{(0)}}^{\tau} d\zeta\, \mathbf{v}_\mathbf{p}(\zeta)\right) \tag{A4}$$

the tunnel exit defined as the coordinate at the time $\Re[t_s'^{(0)}]$:

$$\mathbf{r}_e'^{(0)} = \int_{t_s'^{(0)}}^{\Re[t_s'^{(0)}]} d\zeta\, \mathbf{v}_\mathbf{p}(\zeta) \tag{A5}$$

The second part, $\Delta\mathbf{p}^{(2)}(a)$, does not depend on the boundary. In the following we will show that the first part $\Delta\mathbf{p}^{(1)}(a)$ is negligible under the matching condition $\kappa a \gg 1$. We first note that $\Delta p_y^{(1)}(a)$ is purely imaginary, while $\Delta p_x^{(1)}(a)$ is purely real. In the same geometry that we have used in the main text of the paper $t_a'^{(0)} = i\tau_a'^{(0)}$, and the complex under-the-barrier trajectory is $\mathbf{R} = \mathbf{r} + i\boldsymbol{\rho}$:

$$\mathbf{r} = -a_0\left[\cosh\phi_i'^{(0)} - \cosh\phi\right]\hat{\mathbf{y}} \tag{A6}$$

$$\boldsymbol{\rho} = a_0\left[\frac{\phi}{\phi_i'^{(0)}}\sinh\phi_i'^{(0)} - \sinh\phi\right]\hat{\mathbf{x}} \tag{A7}$$

where $\phi_i'^{(0)} = \omega\tau_i'^{(0)}$ and $\phi = \omega\xi$ and ξ is imaginary integration time variable. The Coulomb potential takes the form (details of the analytical continuation of the Coulomb potential to the complex plane will be addressed in our subsequent publication [19]):

$$U(\mathbf{R}) = -\frac{1}{\sqrt{r^2 - \rho^2}}. \tag{A8}$$

Purely imaginary $\Delta p_y^{(1)}(a)$ is

$$\Delta p_y^{(1)}(a) = -i\int_{\phi_a'^{(0)}}^{0} \frac{r\, d\phi}{\left(r^2 - \rho^2\right)^{3/2}}. \tag{A9}$$

Purely real $\Delta p_x^{(1)}(a)$ is

$$\Delta p_x^{(1)}(a) = \int_{\phi_a'^{(0)}}^{0} \frac{\rho\, d\phi}{\left(r^2-\rho^2\right)^{3/2}}. \tag{A10}$$

and in both cases, $\phi_a = \omega\tau_a'^{(0)}$. Also, since for the optimal trajectory $r \gg \rho$,

$$\Delta p_x^{(1)}(a) \simeq \int_{\phi_a'^{(0)}}^{0} \frac{\rho\, d\phi}{r^3}. \tag{A11}$$

As $\rho = 0$ at the tunnel entrance $\left(\phi = \phi_s'^{(0)} = \omega t_s'^{(0)}\right)$ and $\rho = 0$ at the tunnel exit ($\phi = 0$), the integral is accumulated in the vicinity of $\tau_a'^{(0)}$. We make linear expansion of the integrand around this point:

$$\Delta p_x^{(1)}(a) \simeq v_x'\left(t_s'^{(0)}\right) \int_0^{\tau_a'^{(0)}} d\xi \frac{\tau_a'^{(0)} - \xi}{\left\{\kappa\left(\tau_a'^{(0)} - \xi\right) + a\right\}^3} = C\frac{v_x'\left(t_s'^{(0)}\right)}{\kappa}\frac{1}{\kappa}, \tag{A12}$$

where C is a numerical factor:

$$C = \int_0^{\infty} \frac{z dz}{(z+1)^3}. \tag{A13}$$

So far we have considered $\Delta\mathbf{p}(a)$ defined through its outer region value. We can also estimate $\Delta\mathbf{p}(a)$ using its inner region value. The inner region value of $\Delta\mathbf{p}(a)$ can be calculated using static approximation (or short time propagation), since the time interval from $t_s'^{(0)}$ to $t_a'^{(0)}$ is very small. It is convenient to estimate $\Delta p_y^u(a)$ by evaluating its inner region value. In static field, the momentum in the inner region $p_y^{\text{in}}(a)$ is defined through the energy conservation:

$$-I_p = \frac{\left(p_y^{\text{in}}(a)\right)^2}{2} - \frac{1}{a} - E_0 a \tag{A14}$$

Thus, $p_y^{\text{in}}(a) = -i\sqrt{2(I_p - E_0 a - 1/a)} \simeq -i\sqrt{2(I_p - E_0 a)}(1 + 1/(2a(I_p - E_0 a)))$, yielding $p_y^{\text{in}}(a) = -i\kappa(a) - i/\kappa(a)a$. The first term is the SFA velocity at the boundary $\kappa(a) = \sqrt{2(I_p - E_0 a)} \simeq \kappa$, the second term is the respective correction associated with Coulomb effects. Thus, $\Delta p_y^{\text{in}}(a) \simeq \mathcal{O}(1/\kappa a)$. The vanishingly small value of the correction at the boundary is not surprising, since the boundary is placed in the region, where the Coulomb modification to the barrier is already very small (see Fig. 4).

2. Additional expressions for boundary matching

We derive here the relation:

$$j_\ell\left(a v_{\mathbf{p}^c}\left(t_a'^{(1)}\right)\right) e^{-i\mathbf{r}_s'^{(0)}\cdot\Delta\mathbf{p}} = j_\ell\left(a v_{\mathbf{p}}\left(t_s'^{(0)}\right)\right) \tag{A15}$$

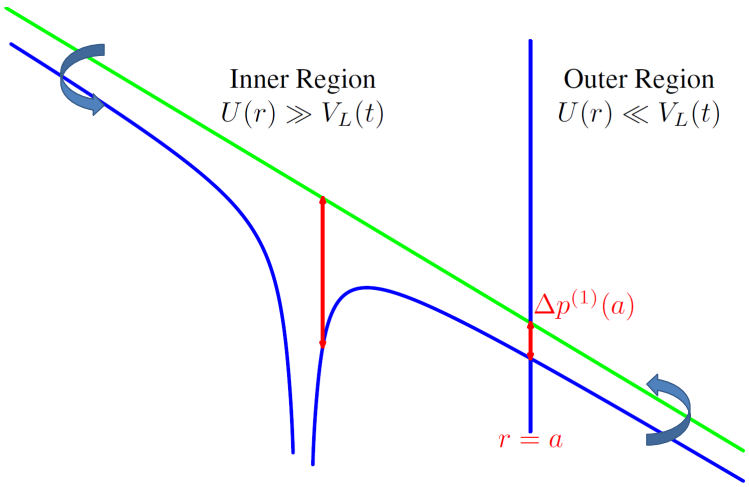

FIG. 4. Cartoon picture of the matching philosophy. As indicated by the two red arrows the imaginary momentum $\Delta p^{(1)}(a)$ is much smaller in the matching region than in the inner region.

Since the saddle point $t_s'^{(1)}$ is close to the SFA saddle point $t_s'^{(0)}$, we know that the argument of j_ℓ is of the order of $\kappa a \gg 1$. So using the large argument approximation for spherical Bessel function, and expanding $v_{\mathbf{p}^c}(t')$ up to first order in $\Delta\mathbf{p}$, we get:

$$j_\ell\left(a v_{\mathbf{p}^c}\left(t_a'^{(1)}\right)\right) = j_\ell\left(a v_{\mathbf{p}}\left(t_a'^{(1)}\right)\right) e^{a\mathbf{v}_{\mathbf{p}}\left(t_a'^{(1)}\right)\cdot\Delta\mathbf{p}/v_{\mathbf{p}}\left(t_a'^{(1)}\right)} \tag{A16}$$

It can be shown that:

$$j_\ell\left(a v_{\mathbf{p}}\left(t_a'^{(1)}\right)\right) = j_\ell\left(a v_{\mathbf{p}}\left(t_a'^{(0)}\right)\right)\left[1 - \frac{a\omega}{\kappa}\Delta t_s'^{(0)}\sqrt{(\zeta^2+\gamma^2)(1+\gamma^2)}\right] \tag{A17}$$

Since the inner region should be treated in quasistatic approximation, the second term is vanishingly small.

Analogously to boundary matching approximation made in [20] we obtain:

$$v_{\mathbf{p}}\left(t_a'^{(0)}\right) \simeq v_{\mathbf{p}}\left(t_s'^{(0)}\right) \tag{A18}$$

Taking into account that by definition

$$\mathbf{r}_s'^{(0)} = a\frac{\mathbf{v}_{\mathbf{p}}\left(t_a'^{(0)}\right)}{v_{\mathbf{p}}\left(t_a'^{(0)}\right)} \tag{A19}$$

and

$$a\frac{\mathbf{v}_{\mathbf{p}}\left(t_a'^{(1)}\right)\cdot\Delta\mathbf{p}}{v_{\mathbf{p}}\left(t_a'^{(1)}\right)} = a\frac{\mathbf{v}_{\mathbf{p}}\left(t_a'^{(0)}\right)\cdot\Delta\mathbf{p}}{v_{\mathbf{p}}\left(t_a'^{(0)}\right)} + \mathcal{O}(G_C^3) \tag{A20}$$

we obtain Eq. (A15). It must be noted that it was because of Eq. (A15) that $j_\ell\left(av_{\mathbf{p}}(t')\right)$ was used in Eq. (31) and not $j_\ell\left(av_{\mathbf{p}^c}(t')\right)$.

Appendix B: Frequency-domain approach

1. The wave-function

In our frequency-domain approach we start the analysis with the expression for the wave-function in the coordinate representation $\psi(\mathbf{r},t) = \langle\mathbf{r}|\psi_{\rm out}(t)\rangle$, where $|\psi_{\rm out}(t)\rangle$ is given by Eq. (5):

$$\psi_{\rm out}(\mathbf{r},t) = i\int_{t_0}^{t} dt' \int d\mathbf{r}' \int d\mathbf{r}''\, \langle\mathbf{r}|U_B(t,t')|\mathbf{r}'\rangle\langle\mathbf{r}'|\hat{L}^-(a)|\mathbf{r}''\rangle\langle\mathbf{r}''|\psi_{\rm in}(t')\rangle \tag{B1}$$

Taking into account the explicit form of the Bloch operator in coordinate representation Eq. (9) we can rewrite Eq. (B1) as follows:

$$\psi(\mathbf{r},t) = i\int_{t_0}^{t} dt' \int d\mathbf{r}' G_B(\mathbf{r},t;\mathbf{r}',t')\delta(r'-a)B(a,\theta',\phi',t') \tag{B2}$$

After following the arguments in subsection III A, we can approximate the boundary term $B(a,\theta',\phi',t')$ as in Eq. (18). This follows from the foresight that when we use the saddle point for the time integral to isolate tunnelling dynamics, we end up with studying the dynamics of the wavefunction around the pole $v(t'_s) = i\kappa$ in the momentum space. This corresponds to prominent contribution only from the asymptotic part of the wavefunction in the region $\kappa r \gg 1$ in co-ordinate space.

Using Eq. (18) and Eq. (25) and evaluating the Delta function over r', we now have for the wavefunction $\psi(\mathbf{r},t)$:

$$\begin{aligned}\psi(\mathbf{r},t) = \frac{i\kappa a^2}{(2\pi)^3}\int_{t_0}^{t} dt' \int d\mathbf{k} \int_0^{\pi} d\theta' \int_0^{2\pi} d\phi'\, e^{i(\mathbf{v_k}(t)\cdot\mathbf{r}-\mathbf{v_k}(t')\cdot\mathbf{a})} e^{-\frac{i}{2}\int_{t'}^{t} d\tau\, v^2(\tau)} \varphi_{\kappa\ell}(a) \\ e^{-i\int_T^t d\tau\, U(\mathbf{r}_L(\tau;\mathbf{r},\mathbf{k},t))+iG_C\left(\mathbf{p},T;\mathbf{r}_s'^{(0)},t'\right)+\left(\mathbf{a}-\mathbf{r}_s'^{(0)}\right)\cdot\nabla G_C\left(\mathbf{p},T;\mathbf{r}_s'^{(0)},t'\right)} N_{\ell m} P_\ell^m(\cos\theta') e^{im\phi'}\end{aligned} \tag{B3}$$

where $N_{\ell m} = \sqrt{\frac{2\ell+1}{4\pi}\frac{(\ell-|m|)!}{(\ell+|m|)!}}$ and $\mathbf{a} = a(\sin\theta'\cos\phi'\,\hat{\mathbf{x}} + \sin\theta'\sin\phi'\,\hat{\mathbf{y}} + \cos\theta'\,\hat{\mathbf{z}})$. We also take $\mathbf{A}(t) = -A_0(\cos\omega t\,\hat{\mathbf{x}} + \sin\omega t\,\hat{\mathbf{y}})$.

The point $\mathbf{r}_s'^{(0)}$ is defined in spherical co-ordinates as $\left(a,\theta_s'^{(0)},\phi_s'^{(0)}\right)$, where $\theta_s'^{(0)} = \theta_v(t')$ and $\phi_s'^{(0)} = \phi_v(t')$, which gives:

$$\mathbf{r}_s'^{(0)} = a\frac{\mathbf{v_k}(t')}{v_{\mathbf{k}}(t')} \approx \int_{t_s'^{(0)}}^{t'} d\tau\, \mathbf{v_k}(\tau) \tag{B4}$$

The approximation follows from the fact that the saddle point for t' will be quite close to the SFA saddle point $t_s'^{(0)}$ and hence by defining $t' - t_s'^{(0)} = \frac{a}{v_{\mathbf{k}}(t')}$, we can redefine saddle point $\mathbf{r}_s'^{(0)}$ as a classical trajectory. t' here corresponds to zeroth order correction in the SFA saddle point when the electron is propagated from a finite boundary instead of the origin (thus the saddle point for $S^{\mathrm{SFA}} + a v_{\mathbf{p}}(t')$).

Following subsection III C, the resulting surface integral is:

$$I_{\Omega'} = \int_0^{\pi} d\theta' \, \sin\theta' \int_0^{2\pi} d\phi' \, e^{-i\mathbf{v}(t')\cdot\mathbf{a}} P_\ell^m(\cos\theta') e^{im\phi'} e^{i\Delta\mathbf{k}\cdot\mathbf{a}} \tag{B5}$$

The term $e^{i\Delta\mathbf{k}\cdot\mathbf{a}}$ comes from the Taylor expansion of the Coulomb phase G_C about the saddle point co-ordinate $\left(a, \theta_s'^{(0)}, \phi_s'^{(0)}\right)$. Since the gradient of G_C is identified as the momentum shift, we can see this term as the contribution of the long-range potential to propagation from the finite boundary $r' = a$. Including this shift by rewriting the shifted kinetic momentum as $\mathbf{v}_{\mathbf{k}^c}(t) = \mathbf{v}_{\mathbf{k}} + \mathbf{A}(t) - \Delta\mathbf{k}$, the integral over ϕ' is evaluated to:

$$\begin{aligned} I_{\phi'} = \int_0^{2\pi} d\phi' \, e^{im\phi'} e^{-i(\mathbf{v}_{\mathbf{k}^c}(t'))\cdot\mathbf{a}} &= \int_0^{2\pi} d\phi' \, e^{im\phi'} e^{-a v_{\mathbf{k}_\rho^c}(t')\sin\theta'\cos(\phi' - \phi_v^c(t')) - a k_z^c \cos\theta'} \\ &= 2\pi e^{im\phi_v^c(t')} J_m\left(a \mathbf{v}_{\mathbf{k}_\rho^c}(t')\sin\theta'\right) e^{-iak_z^c\cos\theta'} \end{aligned}$$

The superscript "c" denotes that we are calculating surface integral over Coulomb shifted momentum and $J_n(z)$ is the nth-order Bessel function of the first kind.

The Ω'-integral now is:

$$I_{\Omega'} = 2\pi(-i)^m e^{im\phi_v^c(t')} \int_0^{\pi} d\theta' \, J_m\left(a v_{\mathbf{k}_\rho^c}(t')\sin\theta'\right) P_\ell^m\left(\cos\theta'\right) e^{-iak_z^c\cos\theta'} \sin\theta' \tag{B6}$$

We depart here from the method used in [10] of approximating the θ'-integral around a given angle according to the direction of polarisation (there, $\theta' \sim \pi$ was a reasonable approximation, and here $\theta' \sim \pi/2$). But with the $\theta' \sim \pi/2$ approximation, not only do we lose accuracy in our result, but the small-argument approximation would not be valid for $J_m(ab\sin\theta')$. But we have used $\theta' \sim \pi/2$ for the Coulomb correction, as deviation from a planar trajectory here is suppressed exponentially [23]. Hence we perform an exact analysis, noting that the above integral has an analytic expression from [24] by using a similar integral on product of Bessel functions and Gegenbauer polynomial from [25], which finally gives us:

$$I_{\Omega'} = 4\pi(-i)^\ell(-1)^m e^{im\phi_v^c(t')} P_\ell^m\left(\frac{k_z^c}{v_{\mathbf{k}^c}(t')}\right) j_\ell\left(a v_{\mathbf{k}^c}(t')\right) \tag{B7}$$

Substituting this result into Eq. (B7) and using Appendix A 2, we get the wavefunction as:

$$\begin{aligned}\psi(\mathbf{r},t) = N_{lm}(-i)^{\ell}(-1)^{m}\varphi(a)\frac{2i\kappa a^2}{(2\pi)^2}\int_{t_0}^{t}dt'\int d\mathbf{k}\, e^{i\mathbf{v}(t)\cdot\mathbf{r}-\frac{i}{2}\int_{t'}^{t}d\tau v^2(\tau)}e^{im\phi_v^c(t')}e^{i\kappa^2(t'-t_0)/2} \\ e^{-i\int_T^t d\tau\, U(\mathbf{r}_L(\tau;\mathbf{r},\mathbf{k},t))+iG_C\left(\mathbf{k},T;\mathbf{r}_s'^{(0)},t'\right)}P_\ell^m\left(\frac{k_z^c}{v_{\mathbf{k}^c}(t')}\right)j_\ell\left(av_{\mathbf{k}}(t')\right)\end{aligned} \tag{B8}$$

Eq. (B8) is an exact expression from ARM under the PPT approximation.

2. Ionisation Rate

In order to calculate the ionisation rate, we need to know the radial current density, $j_\rho(\mathbf{r},t)$, defined as

$$j_\rho(\mathbf{r},t) = \frac{i}{2}\left(\psi(\mathbf{r},t)\frac{\partial\psi^*(\mathbf{r},t)}{\partial\rho} - \psi^*(\mathbf{r},t)\frac{\partial\psi(\mathbf{r},t)}{\partial\rho}\right) \tag{B9}$$

Following the procedure of [14], but noting the changes due to the presence of the Coulomb phase term, we can get the familiar expression:

$$w(\mathcal{E},\omega) = 2\pi\sum_{n\geq n_0}^{\infty}\int d\mathbf{k}\,|F_n(\mathbf{k}^c,\omega)|^2\delta\left[\frac{1}{2}\left(k^2+\kappa^2\left(1+\frac{1}{\gamma^2}\right)\right)-n\omega\right] \tag{B10}$$

with

$$\begin{aligned}F_n(\mathbf{k}^c,\omega) &= \frac{\omega}{2\pi}\int_0^{2\pi}dt'\,F(\mathbf{k}^c,t')e^{in\omega t'} \\ &= \frac{2\kappa a^2}{(2\pi)^{3/2}}(-i)^{\ell}(-1)^m N_{\ell m}\varphi_{\kappa\ell}(a)\int_0^{2\pi}d(\omega t')\,e^{im\phi_v^c(t')}P_\ell^m\left(\frac{k_z^c}{v_{\mathbf{k}^c}(t')}\right) \\ &\quad j_\ell(av_{\mathbf{k}}(t'))e^{-i\frac{k_\rho\kappa}{\omega\gamma}\sin(\omega t'-\phi_k)+in\omega t'}e^{i\int_T^{t'}d\tau\,U\left(\mathbf{r}_L\left(\tau;a,\theta_s'^{(0)},\phi_s'^{(0)},\mathbf{k},t'\right)\right)}\end{aligned} \tag{B11}$$

The Coulomb phase term is the main difference from the result for short range potential.

3. Derivation of $F_n(\mathbf{k},\omega)$

Unlike the result for short-range potentials [14], we now have an additional term in the exponential oscillations due to $j_\ell(av_{\mathbf{k}}(t'))$, along with the Coulomb corrections. Apart from the modified, Coulomb-shifted momentum that is a new result from this analysis, the Coulomb term in the action also includes motion after ionisation, introducing a modification of the result in [8, 14, 22, 26]. As discussed in subsection III E, we know that the saddle

point in time would be such that $v\left(t_a'^{(0)}\right) \approx \pm i\kappa$, and same as done there, can use the asymptotic condition for large argument ($\kappa a \gg 1$) on the spherical Bessel function:

$$j_\ell\left(av_{\mathbf{k}}(t')\right) = \frac{1}{2av_{\mathbf{k}}(t')}\left(e^{i(av_{\mathbf{k}}(t')-(l+1)\pi/2)} + e^{-i(av_{\mathbf{k}}(t')-(l+1)\pi/2)}\right) \tag{B12}$$

The two terms correspond to contributions from the diametrically opposite points on the boundary surface a, from where we propagate the electron outwards. The point farther from the detector by a distance of $2a$ compared to the point nearer causes an additional exponential decay for propagation from the former. Such a term didn't appear in [10], as there saddle-point analysis on $\mathbf{k}$-integral was used, thus isolating the electron field to one particular trajectory, corresponding to a classical particle motion rather than field evolution. Not using saddle-point in our case would naturally lead to inteference effects between the contribution from the two points, but under the given condition ($\kappa a \gg 1$) those effects will be exponentially small. This way, an interference will be produced on every point throughout every circular disc for different θ on the sphere $r' = a$. The contribution of each is weighed by the momentum distribution, encoded in $e^{im\phi_v^c(t')}P_l^m\left(\frac{k_z^c}{v_{\mathbf{k}^c}(t')}\right)$. The maximum contribution comes from the region around the saddle-point, which effectively considers the electron as a particle. However, since our analysis is exact, the contribution from momenta about the classical are also included in the above result, as well as taking into account the case for non-zero perpendicular momentum ($k_z \neq 0$).

The saddle point corresponding to the boundary-dependent action $S_a^{\mathrm{SFA}} = S^{\mathrm{SFA}} + av_{\mathbf{p}}(t')$ can be derived after Taylor expansion about the SFA saddle point $t_s'^{(0)}$:

$$t_a'^{(0)} = t_s'^{(0)} - i\frac{a}{\kappa} \tag{B13}$$

After modifying the SFA saddle point $t_s'^{(0)}$ through the change in $t_a'^{(0)}$ due to the Coulomb phase term, as discussed in section III, we get the final expression for the n-photon transition amplitude, to first order in a:

$$F_n(\mathbf{k},\omega) = \frac{a\varphi(a)}{(2\pi)^{3/2}}(-i)^\ell(-1)^m\sqrt{\frac{2\pi}{\left|S''\left(t_s'^{(0)}\right)\right|}}N_{\ell m}e^{-iS_0\left(t_s'^{(0)}\right)}P_\ell^m\left(\frac{k_z^c}{v_{\mathbf{k}^c}\left(t_s'^{(1)}\right)}\right)e^{im\phi_v^c\left(t_s'^{(1)}\right)}$$
$$j_\ell\left(av_{\mathbf{k}}\left(t_s'^{(1)}\right)\right)e^{i\int_T^{t_a'^{(0)}}d\tau\, U\left(\mathbf{r}_L\left(\tau;a,\theta_s'^{(0)},\phi_s'^{(0)},\mathbf{k},t_s'^{(0)}\right)\right)} \tag{B14}$$

After boundary-matching (subsection III E):

$$F_n(\mathbf{k},\omega) = \frac{C_{\kappa\ell}N_{\ell m}}{2\pi}(-1)^m\left(1+(-1)^{\ell+1}e^{-2\kappa a}\right)\sqrt{\frac{\omega\gamma}{k_\rho\sqrt{\eta^2-1}}}e^{-iS_0\left(t_s'^{(0)}\right)+im\phi_v^c\left(t_s'^{(1)}\right)}$$
$$P_\ell^m\left(\frac{k_z^c}{v_{\mathbf{k}^c}\left(t_s'^{(1)}\right)}\right)e^{-i\int_{t_\kappa'^{(0)}}^{T}d\tau\,U\left(\int_{t_s'}^{\tau}d\zeta\,\mathbf{v}(\zeta)\right)} \tag{B15}$$

Since we are interested in $|F_n(\mathbf{k},\omega)|$ only, we get:

$$|F_n(\mathbf{k},\omega)|^2 = |C_{\kappa\ell}|^2\frac{\omega\gamma}{k_\rho}\frac{2\ell+1}{16\pi^3}\frac{(\ell-|m|)!}{(\ell+|m|)!}\frac{\left(1-(-1)^\ell e^{-2\kappa a}\right)^2}{\sqrt{\eta^2-1}}\left|P_\ell^m\left(\frac{k_z^c}{v_{\mathbf{k}^c}\left(t_s'^{(1)}\right)}\right)\right|^2 \tag{B16}$$
$$e^{-2m\Im\left[\phi_v^c\left(t_s'^{(1)}\right)\right]}e^{-2\frac{A_0k_\rho}{\omega}\left(\eta\cosh^{-1}\eta-\sqrt{\eta^2-1}\right)}e^{2W_{C1}+2W_{C2}}$$

For short-range potentials ($U=0$) the above result matches equation (17) in [8] precisely.

We see another advantage of the ARM here: we now don't have a complicated radial r'-integral and the corresponding higher-order pole in momentum space representation of the wavefunction. The upshot of analysis in short-range potentials [8] was that the pole in the momentum space representation of the wavefunction was cancelled with the zero in the momentum integral at the same point $v(t_s')=i\kappa$. However, for wavefunctions corresponding to long range potentials, we would have had a $Q/\kappa+1$ order pole in the momentum space, leaving a Q/κ order pole in the final momentum integral. Using ARM, the Bloch operator isolates the wavefunction at the boundary $r'=a$ through a delta function, making that integral straightforward, thus bypassing the pole encountered if the integral was performed over the whole radial domain. At the same time we also get a more robust result, taking into account Coulomb correction for the ionisation rate both during and after ionisation.

4. N-Photon Ionisation Rate

The n-photon ionisation rate is

$$\begin{aligned} w_n(\mathcal{E},\omega) &= 2\pi \int d\mathbf{k}\ |F_n(\mathbf{k},\omega)|^2\, \delta\left[\frac{1}{2}\left(k^2+\kappa^2\left(1+\frac{1}{\gamma^2}\right)\right)-n\omega\right] \\ &= |C_{\kappa\ell}|^2\, \omega\kappa \frac{2\ell+1}{8\pi^2}\frac{(\ell-|m|)!}{(\ell+|m|)!}\left(1-(-1)^\ell e^{-2\kappa a}\right)^2 \int_{-\infty}^{\infty} dk_z \int_0^{2\pi} d\phi_k \int_0^{\infty} dk_\rho \\ & e^{-2m\Im\left[\phi_v^c\left(t_s'^{(1)}\right)\right]} \left| P_\ell^m\left(\frac{k_z^c}{v_{\mathbf{k}}\left(t_s'^{(1)}\right)}\right)\right|^2 \frac{e^{-\frac{2A_0k_\rho\eta}{\omega}\left(\tanh^{-1}\sqrt{1-\frac{1}{\eta^2}}-\sqrt{1-\frac{1}{\eta^2}}\right)}}{A_0\eta\sqrt{1-\frac{1}{\eta^2}}} \\ & e^{2W_{C1}+2W_{C2}}\delta\left[\frac{1}{2}\left(k^2+\kappa^2\left(1+\frac{1}{\gamma^2}\right)\right)-n\omega\right] \end{aligned} \tag{B17}$$

Using the Delta function, the integral over k_ρ is easily done by substituting $k_\rho=\sqrt{k_n^2-k_z^2}$, where $k_n^2=2n\omega-\kappa^2\left(1+\frac{1}{\gamma^2}\right)$. We modify the definition of $\zeta=\left(\frac{2n_0}{n}-1\right)$, used in [22] to include contribution from trajectory perpendicular to plane of polarisation to give:

$$\zeta_{\text{eff}} = \frac{2n_0^{\text{eff}}}{n}-1 \tag{B18}$$

where $2n_0^{\text{eff}}\omega=\kappa_{\text{eff}}^2\left(1+\frac{1}{\gamma_{\text{eff}}^2}\right)$, $\kappa_{\text{eff}}^2=\kappa^2+k_z^2$ and $\gamma_{\text{eff}}=\kappa_{\text{eff}}/A_0$ as defined before. The corresponding values for different functions of $\mathbf{k}$ appearing above are as follows:

$$\eta(\mathbf{k}_n) = \sqrt{\frac{1+\gamma_{\text{eff}}^2}{1-\zeta_{\text{eff}}^2}} \tag{B19}$$

$$\sqrt{1-\frac{1}{\eta^2(\mathbf{k}_n)}} = \sqrt{\frac{\zeta_{\text{eff}}^2+\gamma_{\text{eff}}^2}{1+\gamma_{\text{eff}}^2}} \tag{B20}$$

$$\begin{aligned} k_{\rho n} &= \sqrt{n\omega(1-\zeta_{\text{eff}})} \\ A_0 &= \sqrt{\frac{n\omega(1+\zeta_{\text{eff}})}{1+\gamma_{\text{eff}}^2}} \end{aligned} \tag{B21}$$

$$\frac{A_0k_{\rho n}\eta(\mathbf{k}_n)}{\omega} = n = \frac{2n_0^{\text{eff}}}{1+\zeta_{\text{eff}}} = \frac{2n_0}{1+\zeta} \tag{B22}$$

For $k_z \ll k$, we can make the approximation

$$\begin{aligned} \tanh^{-1}\sqrt{1-\frac{1}{\eta^2}}-\sqrt{1-\frac{1}{\eta^2}} &= \frac{1}{2}\ln\frac{1+\sqrt{1-\frac{1}{\eta^2}}}{1-\sqrt{1-\frac{1}{\eta^2}}}-\sqrt{1-\frac{1}{\eta^2}} \\ &\approx \tanh^{-1}\sqrt{\frac{\zeta^2+\gamma^2}{1+\gamma^2}}-\sqrt{\frac{\zeta^2+\gamma^2}{1+\gamma^2}}+\sqrt{\frac{\zeta^2+\gamma^2}{1+\gamma^2}}\frac{k_z^2}{2k_n^2} \end{aligned} \tag{B23}$$

And since we are comparing our result with [8], we make the following approximation on the Coulomb-corrected angle ϕ_v^c: as the corrections Δk_x and Δk_y are generally small, we can expand to first order in these deviations to write ϕ_v^c as a sum of the SFA velocity phase ϕ_v, and a small correction δ defined as:

$$\tan\delta = \frac{\epsilon\tan\phi_v}{1+(1+\epsilon)\tan\phi_v} \tag{B24}$$

where $\epsilon = \frac{\Delta k_x}{v_x} - \frac{\Delta k_y}{v_y}$. This way we can split the exponential $e^{-2m\Im\left[\phi_v^c\left(t_s'^{(1)}\right)\right]}$:

$$e^{-2m\Im\left[\phi_v^c\left(t_s'^{(1)}\right)\right]} = e^{-2m\Im\left[\phi_v\left(t_s'^{(1)}\right)\right]} e^{-2m\Im\left[\delta\left(t_s'^{(1)}\right)\right]} \tag{B25}$$

A further expansion of $\phi_v\left(t_s'^{(1)}\right)$ can be achieved around $\Delta t_s'^{(0)}$ to get:

$$\begin{aligned} e^{-2m\Im\left[\phi_v\left(t_s'^{(1)}\right)\right]} &= e^{-2m\Im\left[\phi_v\left(t_s'^{(0)}\right)\right]} \exp\left[-2m\Im\left\{\frac{\omega\Delta t_s'^{(0)}}{\gamma^2}\left(\frac{\zeta-\gamma^2}{1+\zeta}\right)\right\}\right] \\ &= \left(\frac{k_\rho - A_0 e^{-\cosh^{-1}\eta}}{k_\rho - A_0 e^{\cosh^{-1}\eta}}\right)^m \exp\left[-2m\Im\left\{\frac{\omega\Delta t_s'^{(0)}}{\gamma^2}\left(\frac{\zeta_{\text{eff}}-\gamma_{\text{eff}}^2}{1+\zeta_{\text{eff}}}\right)\right\}\right] \end{aligned} \tag{B26}$$

As the probability of escape of the electron in the direction perpendicular to the field is exponentially supressed, we can make the approximation $k_z \ll k_n$ which gives us:

$$\begin{aligned} \left(\frac{k_\rho - A_0 e^{-\cosh^{-1}\eta}}{k_\rho - A_0 e^{\cosh^{-1}\eta}}\right)^m &\approx \left[\frac{-\zeta-(1-\zeta)\frac{k_z^2}{k_n^2} + \sqrt{\frac{\zeta^2+\gamma^2}{1+\gamma^2}}\left(1+\frac{\varepsilon(k_z)}{2}\right)}{-\zeta-(1-\zeta)\frac{k_z^2}{k_n^2} - \sqrt{\frac{\zeta^2+\gamma^2}{1+\gamma^2}}\left(1+\frac{\varepsilon(k_z)}{2}\right)}\right]^m \\ &= (-1)^{|m|}\left(1+\frac{1}{\gamma^2}\right)^{|m|}\frac{1}{(1-\zeta^2)^{|m|}}\left(\sqrt{\frac{\zeta^2+\gamma^2}{1+\gamma^2}} - \zeta\,\text{sgn}(m)\right)^{2|m|} \end{aligned} \tag{B27}$$

to first order in k_z and $\varepsilon(k_z) = \frac{k_z^2}{k_n^2}\left(\frac{1-\zeta^2}{\gamma^2+\zeta^2}\right)$.

The second term in Eq. (B26) when expanded in powers of k_z has a fourth-order dependence on k_z:

$$\frac{\zeta_{\text{eff}}-\gamma_{\text{eff}}^2}{1+\zeta_{\text{eff}}} = \frac{\zeta-\gamma^2}{1+\zeta}\left(1-\frac{k_z^4}{A_0^2(1+\gamma^2)^2}\right) \tag{B28}$$

Finally, we are left with

$$\begin{aligned} w_n(\mathcal{E},\omega) = |C_{\kappa\ell}|^2 \frac{\kappa}{n}\frac{2\ell+1}{4\pi}\frac{(\ell-|m|)!}{(\ell+|m|)!}\left(1-(-1)^\ell e^{-2\kappa a}\right)^2 \left(\sqrt{\frac{\zeta^2+\gamma^2}{1+\gamma^2}} - \zeta\,\text{sgn}(m)\right)^{2|m|} \\ \left(1+\frac{1}{\gamma^2}\right)^{|m|}\frac{1}{(1-\zeta^2)^{|m|}} e^{-\frac{4n_0}{1+\zeta}\left(\tanh^{-1}\sqrt{\frac{\zeta^2+\gamma^2}{1+\gamma^2}} - \sqrt{\frac{\zeta^2+\gamma^2}{1+\gamma^2}}\right)}\sqrt{\frac{1+\gamma^2}{\zeta^2+\gamma^2}} e^{-2m\Im\left[\delta\left(t_s'^{(1)}\right)\right]} \\ e^{-2m\frac{\zeta-\gamma^2}{1+\zeta}\Im\left[\frac{\omega\Delta t_s'^{(0)}}{\gamma^2}\right]} e^{2W_{C1}+2W_{C2}} \int_{-k_n}^{k_n} dk_z\, e^{-\frac{2n_0}{1+\zeta}\sqrt{\frac{\zeta^2+\gamma^2}{1+\gamma^2}}\frac{k_z^2}{k_n^2}} \left|P_\ell^m\left(\frac{k_z}{\pm i\kappa}\right)\right|^2 \end{aligned} \tag{B29}$$

upto second order in k_z. The Coulomb correction is taken out of the integral, on account of its extremely weak dependence on the k_z-component of the momentum. The above result is valid for all values of ℓ and m. An m-dependent correction due to the Coulomb potential is also seen to manifest through its effect on the SFA saddle point $t_s'^{(0)}$.

To compare with [8], we conisder the case of $\ell = 1, m = \pm 1$, for which we have $P_\ell^m\left(\frac{k_z}{\pm i\kappa}\right) = -\sqrt{1+\frac{k_z^2}{\kappa^2}}$. To first approximation, we ignore the $\frac{k_z^2}{\kappa^2}$ term in the prefactor, and note that since $n \gg 1$, we can approximate the integral as:

$$\int_{-k_n}^{k_n} dk_z\, e^{-n\sqrt{\frac{\zeta^2+\gamma^2}{1+\gamma^2}}\frac{k_z^2}{k_n^2}} \approx \int_{-\infty}^{\infty} dk_z\, e^{-n\sqrt{\frac{\zeta^2+\gamma^2}{1+\gamma^2}}\frac{k_z^2}{k_n^2}} = k_n\sqrt{\frac{\pi}{n}}\left(\frac{1+\gamma^2}{\zeta^2+\gamma^2}\right)^{1/4} \tag{B30}$$

which gives

$$\begin{aligned} w_n(\mathcal{E},\omega) = \frac{3\left|C_{\kappa l}\right|^2 I_p}{8\sqrt{2\pi}n_0^{3/2}}\frac{e^{2(W_{C1}+W_{C2})}}{\sqrt{1-\zeta}} e^{-\frac{4n_0}{1+\zeta}\left(\tanh^{-1}\sqrt{\frac{\zeta^2+\gamma^2}{1+\gamma^2}}-\sqrt{\frac{\zeta^2+\gamma^2}{1+\gamma^2}}\right)} e^{-2m\Im\left[\delta\left(t_s'^{(1)}\right)\right]} \\ e^{-2m\frac{\zeta-\gamma^2}{1+\zeta}\Im\left[\frac{\omega\Delta t_s'^{(0)}}{\gamma^2}\right]}\left(1+\frac{1}{\gamma^2}\right)^{3/2}\left(\frac{1+\gamma^2}{\zeta^2+\gamma^2}\right)^{3/4}\left(\sqrt{\frac{\zeta^2+\gamma^2}{1+\gamma^2}}-\zeta\,\mathrm{sgn}(m)\right)^2 \end{aligned} \tag{B31}$$

The main difference from Eq. (19) of [8] is incorporation of Coulomb correction, starting from the tunnelling region and into the continuum until the electron is registered at the detector, and an orbital dependent Coulomb-correction, a result that wasn't expected.

Eq. (B31) is equivalent to Eq. (70) obtained within time-domain approach. However, here we have a result that is valid beyond the optimal momentum, whereas in Eq. (70) we have effectively derived the total ionisation rate summed over all photon orders, which is to be compared with Eq. (6) of [8]. For Eq. (B31), further discussion on its range requires a knowledge of $\Delta\mathbf{p}$ over all $\mathbf{p}$, and will be considered elsewhere.

Appendix C: Subcycle ionisation amplitude

We now consider the case of subcycle ionisation amplitudes in time domain, to replace $T \to t$. The sub-cycle ionisation amplitude is defined as:

$$a_{\mathbf{p}}(t) = i\int_{\mathbf{a}} d\mathbf{r}\,\langle \mathbf{p}+\mathbf{A}(t)|\mathbf{r}\rangle\psi(\mathbf{r},t) \tag{C1}$$

Back-propagating the solution $\psi(\mathbf{r},T)$, we can write $\psi(\mathbf{r},t)$ as:

$$\psi(\mathbf{r},t) = \int_{\mathbf{a}} d\mathbf{r}'\,G(\mathbf{r},t;\mathbf{r}',T)\psi(\mathbf{r}',T) - i\int_T^t dt'\int_{\mathbf{a}} d\mathbf{r}'\,G(\mathbf{r},t;\mathbf{r}',t')\delta(r'-a)B(a,\theta',\phi',t') \tag{C2}$$

The second term represents that part of the wavefunction that remains bounded within the confines of the Coulomb potential near the atom after ionisation. But the wavefunction content in that region after ionisation is negligible compared to the current flux in continnum, thus making the contribution from the former almost zero. So we can write equation (C1) as:

$$\begin{aligned} a_{\mathbf{p}}(t) &= i\int_{\mathbf{a}} d\mathbf{r}\,\langle \mathbf{p}+\mathbf{A}(t)|\mathbf{r}\rangle \int_{\mathbf{a}} d\mathbf{r}'\, G^{\mathrm{EVA}}(\mathbf{r},t;\mathbf{r}',T)\psi(\mathbf{r}',T) \\ &= i\int_{\mathbf{a}} d\mathbf{r}\int_{\mathbf{a}} d\mathbf{r}'\int d\mathbf{k}\,\frac{e^{-i(\mathbf{p}+\mathbf{A}(t))\cdot\mathbf{r}}}{(2\pi)^{3/2}}\frac{e^{i(\mathbf{k}+\mathbf{A}(t))\cdot\mathbf{r}-i\mathbf{k}\cdot\mathbf{r}'}}{(2\pi)^3}e^{-i\int_T^t d\tau\, U(\mathbf{r}_L(\tau;\mathbf{r},\mathbf{p},t))} \\ & e^{-\frac{i}{2}\int_{t'}^t d\tau\, v^2(\tau)}\psi(\mathbf{r}',T) \\ &= \frac{1}{(2\pi)^3}\int_{\mathbf{a}} d\mathbf{r}\int d\mathbf{k}\, e^{i(\mathbf{k}-\mathbf{p}-\Delta\mathbf{p})\cdot\mathbf{r}-\frac{i}{2}\int_T^t d\tau\, v_{\mathbf{k}}^2(\tau)}e^{-i\int_T^t d\tau\, U(\mathbf{r}_L(\tau;\mathbf{r},\mathbf{k},t))}a_{\mathbf{k}}(T) \end{aligned}$$

Before we can perform the integration on $\mathbf{r}$, we need to address the $(\mathbf{r},\mathbf{k})$-dependence of the Coulomb correction in the above equation. Similar to section III, we will expand the Coulomb phase term $G_C(\mathbf{k},T;\mathbf{r},t) = \int_T^t d\tau\, U\left(\mathbf{r}+\int_t^\tau d\zeta\,\mathbf{v}_{\mathbf{k}}(\zeta)\right)$, about the appropriate saddle point $\mathbf{r}_s$ upto quadratic terms in deviation $(\mathbf{a}-\mathbf{r}_s)$. We need the saddle point for the phase term:

$$S^{\mathrm{SFA}}(\mathbf{r},\mathbf{k},t) = (\mathbf{k}-\mathbf{p})\cdot\mathbf{r} - \frac{1}{2}\int_{t_s'}^t d\tau\, v_{\mathbf{k}}^2(\tau) \tag{C3}$$

Therefore,

$$\nabla_{\mathbf{k}} S^{\mathrm{SFA}} = \mathbf{r} - \int_{t_s'}^t d\tau\,\mathbf{v}_{\mathbf{k}}(\tau) = 0 \tag{C4}$$

and

$$\nabla_{\mathbf{r}} S^{\mathrm{SFA}} = \mathbf{k}-\mathbf{p} = 0 \tag{C5}$$

So the classical trajectory can be written as:

$$\mathbf{r}_s = \int_{t_s'}^t d\tau\,\mathbf{v}_{\mathbf{p}}(\tau) \tag{C6}$$

After expanding the Coulomb phase term $G_C(\mathbf{k},T;\mathbf{r},t)$ about the saddle points $(\mathbf{r}_s,\mathbf{k}_s)$ as in section III, we can write the subcycle transition amplitude as:

$$a_{\mathbf{p}}(t) = \frac{1}{(2\pi)^3}\int d\mathbf{k}\int d\mathbf{r}\, e^{i(\mathbf{k}-\mathbf{p})\cdot\mathbf{r}-\frac{i}{2}\int_T^t d\tau\, v_{\mathbf{k}}^2(\tau)-iG_C(\mathbf{p},T;\mathbf{r}_s,t)-i(\mathbf{r}-\mathbf{r}_s)\cdot\nabla G_C(\mathbf{p},T;\mathbf{r}_s,t)}a_{\mathbf{k}}(T) \tag{C7}$$

Note the subscript $\mathbf{p}$ in G_C: the phase term is evaluated for the asymptotic momentum $\mathbf{p}$ and hence the corresponding momentum shift from this Taylor-expansion $\Delta\mathbf{p} = \nabla G_C$ is

also evaluated for the asymptotic momentum $\mathbf{p}$ and not for the intermediate momentum $\mathbf{k}$ on which we have to perform the integration.

We also have achieved the conventional ad-hoc method used to calculate momentum shifts [23], into a rigorous anaylsis arising from stationary points of the EVA action. Following our analysis, we first propagate the electron till the detector after ionisation, and to find the momentum shifts at any point of time during this motion, we propagate it back through the EVA Green's function and thus have information on sub-cycle momentum shifts also.

We can now write,

$$\int_T^t d\tau\, U\left(\mathbf{r}+\int_t^\tau d\zeta\, \mathbf{v}_{\mathbf{k}}(\zeta)\right)\Big|_{\mathbf{r}=\mathbf{r}_s,\mathbf{k}_s=\mathbf{p}} = \int_T^t d\tau\, U\left(\int_{t_s'}^\tau d\zeta\, \mathbf{v}_{\mathbf{p}}(\zeta)\right) \tag{C8}$$

And we can combine this with:

$$\int_T^{t_\kappa'^{(0)}} d\tau\, U\left(\int_{t_s'^{(0)}}^\tau d\zeta\, \mathbf{v}(\zeta)\right) \tag{C9}$$

in $a_{\mathbf{p}}(T)$ Eq. (36), to get:

$$\int_T^t d\tau\, U\left(\int_{t_s'^{(0)}}^\tau d\zeta\, \mathbf{v}(\zeta)\right) + \int_{t_\kappa'^{(0)}}^T d\tau\, U\left(\int_{t_s'^{(0)}}^\tau d\zeta\, \mathbf{v}(\zeta)\right) = \int_{t_\kappa'^{(0)}}^t d\tau\, U\left(\int_{t_s'^{(0)}}^\tau d\zeta\, \mathbf{v}(\zeta)\right) \tag{C10}$$

which solves the Coulomb correction for $a_{\mathbf{p}}(t)$. The integral on $\mathbf{k}$ this time gives $\mathbf{k} = \mathbf{p}+\Delta\mathbf{p}(t,T)$. The $\mathbf{r}$-integral now is straightforward to calculate, and we finally get:

$$\begin{aligned} a_{\mathbf{p}}(t) = (-1)^{m+1} C_{\kappa\ell} N_{\ell m} \sqrt{\frac{\gamma}{\omega p_\rho \sqrt{\eta^2-1}}} e^{-i\int_{t_\kappa'^{(0)}}^t d\tau\, U\left(\int_{t_s'}^\tau d\zeta\, \mathbf{v}_{\mathbf{p}}(\zeta)\right)} e^{-\frac{i}{2}\int_{t_s'^{(0)}}^t d\tau\, v^2_{\mathbf{p}+\Delta\mathbf{p}}(\tau)} \\ e^{i\kappa^2 t_s'^{(0)}/2} e^{i\mathbf{r}_s\cdot\Delta\mathbf{p}} P_\ell^m\left(\frac{p_z^c}{v_{\mathbf{p}^c}\left(t_s'^{(1)}\right)}\right) e^{im\phi_v^c\left(t_s'^{(1)}\right)} \end{aligned} \tag{C11}$$

where we have ignored corrections of the order of $\mathcal{O}(G_C^2)$ and greater, which would arise from the Coulomb phase and the Coulomb-shifted velocity phase ϕ_v^c after taking $\mathbf{k} = \mathbf{p}+\Delta\mathbf{p}(t,T)$. Expanding $\int_{t_s'^{(0)}}^t d\tau\, v^2_{\mathbf{p}+\Delta\mathbf{p}}(\tau)$ upto first order in $\Delta\mathbf{p}$, it will cancel the spurious term $\mathbf{r}_s\cdot\Delta\mathbf{p}$. Also $\mathbf{p}^c$ is defined as $\mathbf{p}^c = \mathbf{p}-\Delta\mathbf{p}(t_\kappa'^{(0)},t)$. The final expression for sub-cycle transition amplitude is:

$$\begin{aligned} a_{\mathbf{p}}(t) = (-1)^{m+1} C_{\kappa\ell} N_{\ell m} \sqrt{\frac{\gamma}{\omega p_\rho \sqrt{\eta^2-1}}} e^{-i\int_{t_\kappa'^{(0)}}^t d\tau\, U\left(\int_{t_s'}^\tau d\zeta\, \mathbf{v}_{\mathbf{p}}(\zeta)\right)} e^{-\frac{i}{2}\int_{t_s'^{(0)}}^t d\tau\, v^2_{\mathbf{p}}(\tau)+i\kappa^2 t_s'^{(0)}/2} \\ P_\ell^m\left(\frac{p_z^c}{v_{\mathbf{p}^c}\left(t_s'^{(1)}\right)}\right) e^{im\phi_v^c\left(t_s'^{(1)}\right)} \end{aligned} \tag{C12}$$

Appendix D

We derive here the result

$$\lim_{\rho\to\infty} \frac{\rho J_1(\rho d(\mathbf{k}_\rho, \mathbf{p}_\rho))}{d(\mathbf{k}_\rho, \mathbf{p}_\rho)} = 2\pi\delta(\mathbf{k}_\rho - \mathbf{p}_\rho) \tag{D1}$$

We start from the integral

$$I_\rho = \int_0^{2\pi} d\phi \int_0^\rho d\rho'\, \rho' e^{i(\mathbf{k}_\rho - \mathbf{p}_\rho)\cdot\rho'} \tag{D2}$$

This integral can be written as:

$$\begin{aligned} I_\rho &= \int_0^{2\pi} d\phi \int_0^\rho d\rho'\, \rho' e^{i(k_\rho \rho' \cos(\phi-\phi_k) - p_\rho \rho' \cos(\phi-\phi_p))} \\ &= \int_0^{2\pi} d\phi \int_0^\rho d\rho'\, \rho' \sum_{n_1=-\infty}^{\infty} i^{n_1} J_{n_1}(k_\rho\rho') e^{in_1(\phi-\phi_k)} \sum_{n_2=-\infty}^{\infty} (-i)^{n_2} J_{n_2}(p_\rho\rho') e^{-in_2(\phi-\phi_k)} \\ &= 2\pi \int_0^\rho d\rho'\, \rho' J_0(\rho' d(\mathbf{k}_\rho, \mathbf{p}_\rho)) \end{aligned}$$

In going from step two to three, we first perform the integral over ϕ and then use the Graf generalisation of Neumann summation. The integral over ρ' is simple

$$\int_0^\rho d\rho'\, \rho' J_0(\mathbf{k}_\rho, \mathbf{p}_\rho) = \frac{\rho J_1(\rho d(\mathbf{k}_\rho, \mathbf{p}_\rho))}{d(\mathbf{k}_\rho, \mathbf{p}_\rho)} \tag{D3}$$

Therefore

$$I_\rho = 2\pi \frac{\rho J_1(\rho d(\mathbf{k}_\rho, \mathbf{p}_\rho))}{d(\mathbf{k}_\rho, \mathbf{p}_\rho)} \tag{D4}$$

Now, by definition

$$\begin{aligned} (2\pi)^2\delta(\mathbf{k}_\rho - \mathbf{p}_\rho) &= \int_0^{2\pi} d\phi \int_0^\infty d\rho'\, \rho' e^{i(\mathbf{k}_\rho - \mathbf{p}_\rho)\cdot\rho'} \\ &= \lim_{\rho\to\infty} \int_0^{2\pi} d\phi_k \int_0^\rho d\rho'\, \rho' e^{i(\mathbf{k}_\rho - \mathbf{p}_\rho)\cdot\rho'} \\ &= \lim_{\rho\to\infty} 2\pi \frac{\rho J_1(\rho d(\mathbf{k}_\rho, \mathbf{p}_\rho))}{d(\mathbf{k}_\rho, \mathbf{p}_\rho)} \end{aligned}$$

And we get

$$\lim_{\rho\to\infty} \frac{\rho J_1(\rho d(\mathbf{k}_\rho, \mathbf{p}_\rho))}{d(\mathbf{k}_\rho, \mathbf{p}_\rho)} = 2\pi\delta(\mathbf{k}_\rho - \mathbf{p}_\rho) \tag{D5}$$

which is the desired result.

Appendix E

We establish the relation

$$e^{im\phi_k}\left(\frac{k_\rho - A_0 e^{-i(\phi_k-\omega t)}}{k_\rho - A_0 e^{i(\phi_k-\omega t)}}\right)^{m/2} = e^{im\phi_v(t)} \tag{E1}$$

where $\phi_v(t) = \tan^{-1}\frac{v_y(t)}{v_x(t)}$. We can write

$$\begin{aligned}\phi_v(t) &= \tan^{-1}\left(\frac{k_\rho \sin\phi_k - A_0 \sin\omega t}{k_\rho\cos\phi_k - A_0\cos\omega t}\right)\\ &= \tan^{-1}\left[\frac{k_\rho e^{i\phi_k} - A_0 e^{i\omega t} - \left(k_\rho e^{-i\phi_k} - A_0 e^{-i\omega t}\right)}{i\left(k_\rho e^{i\phi_k} - A_0 e^{i\omega t} + k_\rho e^{-i\phi_k} - A_0 e^{-i\omega t}\right)}\right]\end{aligned} \tag{E2}$$

Taking $\Phi = \left(\frac{k_\rho e^{i\phi_k} - A_0 e^{\omega t}}{k_\rho e^{-i\phi_k} - A_0 e^{-i\omega t}}\right)$, we get

$$\begin{aligned}\phi_v(t) = \tan^{-1}\left[i\frac{1-\Phi}{1+\Phi}\right] &= i\tanh^{-1}\left(\frac{1-\Phi}{1+\Phi}\right)\\ &= \frac{i}{2}\ln\left[\frac{1+\frac{1-\Phi}{1+\Phi}}{1-\frac{1-\Phi}{1+\Phi}}\right]\\ &= -\frac{i}{2}\ln\Phi = -\frac{i}{2}\ln\left(\frac{k_\rho e^{i\phi_k} - A_0 e^{i\omega t}}{k_\rho e^{-i\phi_k} - A_0 e^{-i\omega t}}\right)\end{aligned}$$

Therefore,

$$\begin{aligned}e^{im\phi_v(t)} &= \exp\left[\frac{m}{2}\ln\left(\frac{k_\rho e^{i\phi_k} - A_0 e^{i\omega t}}{k_\rho e^{-i\phi_k} - A_0 e^{-i\omega t}}\right)\right]\\ &= \left(\frac{k_\rho e^{i\phi_k} - A_0 e^{i\omega t}}{k_\rho e^{-i\phi_k} - A_0 e^{-i\omega t}}\right)^{m/2} = e^{im\phi_k}\left(\frac{k_\rho - A_0 e^{-i(\phi_k-\omega t)}}{k_\rho - A_0 e^{i(\phi_k-\omega t)}}\right)^{m/2}\end{aligned} \tag{E3}$$

which is the required result.

---

[1] P. Eckle, M. Smolarski, P. Schlup, J. Biegert, A. Staudte, M. Schöffler, H. G. Muller, R. Dörner, and U. Keller, Nat. Phys. **4**, 565 (2008).

[2] P. Eckle, A. N. Pfeiffer, C. Cirelli, A. Staudte, R. Dörner, H. G. Muller, M. Büttiker, and U. Keller, Science **322**, 1525 (2008).

[3] A. N. Pfeiffer, C. Cirelli, M. Somlarski, R. Dörner, and U. Keller, Nat. Phys. **7**, 428 (2011).

[4] A. N. Pfeiffer, C. Cirelli, M. Molarski, D. Dimitriovski, M. Abu-samha, L. B. Madsen, and U. Keller, Nat. Phys. **8**, 76 (2012).

[5] H. Akagi, T. Otobe, A. Staudte, A. Shiner, F. Turner, R. Dörner, D. M. Villeneuve, and P. B. Corkum, Science **325**, 1364 (2009).

[6] A. Fleischer, H. J. Wörner, L. Arissian, L. R. Liu, M. Meckel, A. Rippert, R. Dörner, D. M. Villeneuve, P. B. Corkum, and A. Staudte, Phys. Rev. Lett. **107**, 113003 (2011).

[7] L. D. Landau and E. M. Lifshitz, *Course of Theoretical Physics*, 2nd ed., Vol. 3 (Pergamon Press, 1977).

[8] I. Barth and O. Smirnova, Phys. Rev. A **84**, 063415 (2011).

[9] R. Torres, T. Siegel, L. Brugnera, I. Procino, J. G. Underwood, C. Altrucci, R. Velotta, E. Springale, C. Froud, I. C. E. Turcu, M. Yu. Ivanov, O. Smirnova, and J. P. Marangos, Opt. Express **18**, 3174 (2010).

[10] L. Torlina and O. Smirnova, Phys. Rev. A (2012).

[11] L. Torlina, M. Yu. Ivanov, Z. B. Walters, and O. Smirnova, Phys. Rev. A (2012).

[12] P. G. Burke, *R-Matrix Theory of Atomic Collisions*, Vol. 61 (Springer Series on Atomic, Optical and Plasma Physics, 2011).

[13] M. A. Lysaght, L. R. Moore, L. A. A. Nikolopoulos, J. S. Parker, H. W. van der Hart, and K. T. Taylor, *Quantum Dynamics Imaging: Theoretical and Numerical Methods* (2011) pp. 107–134.

[14] A. M. Perelomov, V. S. Popov, and M. V. Terentév, Sov. Phys. JETP **23**, 924 (1966).

[15] S. V. Popruzhenko, V. D. Mur, V. S. Popov, and D. Bauer, Phys. Rev. Lett. **101**, 193003 (2008).

[16] O. Smirnova, M. Spanner, and M. Ivanov, Phys. Rev. A **77**, 033407 (2008).

[17] O. Smirnova, M. Spanner, and M. Ivanova, J. Phys. B **39**, S307 (2006).

[18] O. Smirnova, A. S. Mouritzen, S. Patchkovskii, and M. Yu. Ivanov, J. Phys. B **40**, F197 (2007).

[19] L. Torlina, J. Kaushal, and O. Smirnova, in preparation.

[20] R. Murray, W. K. Liu, and M. Yu. Ivanov, Phys. Rev. A **81**, 023413 (2010).

[21] I. Barth and O. Smirnova, Phys. Rev. A **87**, 013433 (2013).

[22] A. M. Perelomov, V. S. Popov, and M. V. Terentév, Sov. Phys. JETP **24**, 207 (1967).

[23] V. S. Popov, Phys.-Usp. **47**, 9 (2004).

[24] B. Podolsky and L. Pauling, Phys. Rev. **34**, 109 (1929).

[25] G. N. Watson, *A Treatise on the Theory of Bessel Functions* (Cambridge University Press, 1922).

[26] A. M. Perelomov and V. S. Popov, Sov. Phys. JETP **25**, 336 (1967).